EUROPEAN ORGANIZATION FOR NUCLEAR RESEARCH (CERN)

CERN-EP-2026-092
2026/09/09

CMS-EGM-24-002

Highly boosted dielectron identification in proton-proton collisions at $\sqrt{s} = 13\,\text{TeV}$

The CMS Collaboration*

arXiv:2604.13320v2 [hep-ex] 8 Sep 2026

Abstract

A new technique is developed to identify dielectrons (e^+e^-) with Lorentz boost $\gamma_L > 20$ that produce one single merged cluster in the electromagnetic calorimeter of the CMS detector. The identification uses two multivariate models: one for the case where both electron tracks are reconstructed, and another where only one of the tracks is reconstructed. The efficiency is determined using proton-proton collision data collected at a center-of-mass energy of 13 TeV. Boosted J/ψ mesons decaying into e^+e^- pairs are used to estimate the efficiency of the model with two tracks, yielding an overall efficiency of 80%. The $Z \to \mu^+\mu^-\gamma$ events, where the photon converts into a collimated dielectron, are used for the model with a single track, yielding an efficiency of about 60%. A dedicated energy correction for dielectron candidates is also developed using $B^\pm \to J/\psi K^\pm \to e^+e^-K^\pm$ data.

Published in Physical Review D as doi:10.1103/hb72-vjj6.

© 2026 CERN for the benefit of the CMS Collaboration. CC-BY-4.0 license

*See Appendix A for the list of collaboration members

1 Introduction

The electron and photon reconstruction and identification (ID) techniques developed by the CMS Collaboration at the CERN LHC provide excellent energy resolution and efficiency, and their performance was rigorously demonstrated using LHC Run 2 proton-proton collision data at $\sqrt{s} = 13\,\text{TeV}$ collected during 2016–2018 [1], corresponding to an integrated luminosity of $138\,\text{fb}^{-1}$. The techniques are designed to deliver the best possible performance for the well-isolated prompt electrons and photons typically used in precision measurements of standard model (SM) processes and in many searches for physics beyond the SM (BSM).

However, numerous BSM models predict light bosons associated with new heavy resonances, which may subsequently decay into a dielectron (e^+e^-) [2–4], whose angular separation can be small. This can make the individual identification of each electron difficult when the opening angle is similar or smaller than the calorimeter granularity or the size of its effective Molière radius. Also, in order to obtain the best possible energy resolution, electron reconstruction algorithms are designed to identify associated bremsstrahlung photons near electron candidates and include them in the electron energy. This can result in the merging of two nearby electrons.

In this paper, we present an algorithm for Run 2 data to identify merged electrons (e_{ME}) with an arbitrary dielectron invariant mass, m_{ee}. The CMS Collaboration has previously developed algorithms to identify merged photon clusters [5, 6] using images of the energy deposits recorded in the calorimeter. The ATLAS Collaboration has previously developed an algorithm to identify e_{ME} from the decay of highly boosted on-shell Z bosons with $60 < m_{\text{ee}} < 120\,\text{GeV}$ [7].

The algorithm has two types of e_{ME}, with ("two-track") and without ("single-track") a secondary associated track. Each type is identified with its own multivariate model. The two-track model relies on the geometrical compatibility between the merged cluster and the two electron tracks. Its efficiency is validated using boosted J/ψ mesons decaying to e^+e^- since they provide an abundant number of e^+e^- pairs with Lorentz boost $\gamma_{\text{L}} > 20$, in contrast to the Z boson that requires about 2 TeV of energy to reach the same level of γ_{L}. The single-track model mainly utilizes the ratio between the merged cluster's energy and the electron track's momentum. Its efficiency is measured using $\text{Z} \to \mu^+\mu^-\gamma$ events with a photon conversion, because the e^+e^- pair from a converted photon often has only a single track reconstructed due to the insufficient separation, mimicking the feature of the single-track e_{ME}. For the two-track model, a dedicated energy correction is also developed to match the energy description of the merged cluster in simulation to that in data. As the cluster from $\text{J}/\psi \to \text{e}^+\text{e}^-$ is merged, $\text{B}^\pm \to \text{J}/\psi\text{K}^\pm \to \text{e}^+\text{e}^-\text{K}^\pm$ decays are used to construct a resonance structure to derive the energy scale and resolution of the merged cluster. The method described in this paper is used to identify e_{ME} produced in the decay of a hypothetical light BSM boson in data collected by the CMS detector [8]. The new e_{ME} ID significantly improves the sensitivity in the electron channel within the phase space with Lorentz boost $\gamma_{\text{L}} > 20$ by reducing backgrounds originating from isolated single electrons.

2 The CMS detector

The CMS apparatus [9, 10] is a multipurpose, nearly hermetic detector, designed to trigger on [11–13] and identify electrons, muons, photons, and (charged and neutral) hadrons [1, 14, 15]. Its central feature is a superconducting solenoid of 6 m internal diameter, providing a magnetic field of 3.8 T. Within the solenoid volume are a silicon pixel and strip tracker, a lead tungstate crystal electromagnetic calorimeter (ECAL), and a brass and scintillator hadron calorimeter (HCAL), each composed of a barrel and two endcap sections.

The silicon tracker used in 2016 measured charged particles within the pseudorapidity range $|\eta| < 2.5$. The pixel tracker had three (four) barrel layers and two (three) disks on each endcap region in 2016 (2017 and 2018) [16]. The strip tracker has ten layers in the barrel region with four layers in the tracker inner barrel and six layers in the tracker outer barrel. The inner barrel is supplemented with three tracker inner disks at each end. The strip tracker endcap consists of nine disks that cover up to $|\eta| < 2.5$.

The ECAL consists of 75 848 lead tungstate crystals, which provide coverage in $|\eta| < 1.48$ in a barrel region (EB) and $1.48 < |\eta| < 3.0$ in two endcap regions (EE). The EB is divided by 360 in azimuthal angle ϕ and 170 in η. Each crystal's size corresponds to 0.0174×0.0174 in $\eta \times \phi$ or $22 \times 22\,\mathrm{mm}^2$ at the front face of the crystal and $26 \times 26\,\mathrm{mm}^2$ at the rear face. The Molière radius of lead tungstate is 22 mm. The crystal length is 230 mm, corresponding to 25.8 radiation lengths (X_0). The centers of the front faces are located at a 1.29 m cylindrical radius from the beam axis. Preshower detectors consisting of two planes of silicon sensors interleaved with a total of $3X_0$ of lead are located in front of each EE detector. The HCAL barrel (HB) has a symmetric 72-fold segmentation in the ϕ direction and 32-fold in η. Each HB tower has a lateral dimension of 0.087×0.087 in $\eta \times \phi$. The inner radius of the HB is approximately 1.8 m. Forward calorimeters extend the pseudorapidity coverage provided by the barrel and endcap detectors. Muons are reconstructed in gas-ionization detectors embedded in the steel flux-return yoke outside the solenoid. A more detailed description of the CMS detector, together with a definition of the coordinate system used and the relevant kinematic variables, can be found in Refs. [9, 10].

A particle-flow (PF) algorithm [17] aims to reconstruct and identify each individual particle in an event, with an optimized combination of information from the various elements of the CMS detector. The charged-particle trajectory reconstruction is seeded by two or three consecutive hits in the pixel tracker. The trajectory finding and fitting are performed by the Kalman filter (KF) algorithm, which extrapolates the seed trajectory to the next layer along the expected trajectory. It uses the most compatible hit in the next layer to update the trajectory state iteratively [15]. The energy of photons is obtained from the ECAL measurement. The energy of electrons is determined from a combination of the electron momentum at the primary interaction vertex (PV), as determined by an alternative track reconstruction using the Gaussian sum filter (GSF) algorithm [18], the energy of the corresponding ECAL cluster, and the energy sum of all bremsstrahlung photons spatially compatible with originating from the electron track. The energy of muons is obtained from the curvature of the corresponding KF track. The energy of charged hadrons is determined from a combination of their KF track momenta and the matching ECAL and HCAL energy deposits, corrected for the calorimeter response to hadronic showers. Finally, the energy of neutral hadrons is obtained from the corresponding corrected ECAL and HCAL energies.

For the standard reconstruction algorithm, the electron momentum resolution for electrons with the transverse momentum $p_\mathrm{T} \approx 45\,\mathrm{GeV}$ from $\mathrm{Z} \to \mathrm{e}^+\mathrm{e}^-$ decays ranges from 1.6 to 5%. It is generally better in the barrel region than in the endcaps, and also depends on the bremsstrahlung energy emitted by the electron as it traverses the material in front of the ECAL [1, 19].

Events of interest are selected using a two-tiered trigger system. The first level (L1), composed of custom hardware processors, uses information from the calorimeters and muon detectors to select events at a rate of around 100 kHz within a fixed latency of $4\,\mu$s [11]. The second level, known as the high-level trigger, consists of a farm of processors running a version of the full event reconstruction software optimized for fast processing, and reduces the event rate to a few

1 kHz before data storage [12].

3 Simulated events

To study the signature of highly boosted dielectron pairs originating from potential BSM processes, signal events are generated using the PYTHIA 8.240 Monte Carlo (MC) event generator [20] with benchmark models $pp \to X \to YY \to 4e$, where X and Y are bosons with $m_X = 250, 750, 2000\,\text{GeV}$ and $m_Y = 1, 10\,\text{GeV}$. Physics processes containing isolated electrons are used for backgrounds. The W boson production, Drell-Yan (DY), and $t\bar{t}$ pair production processes are generated using the MADGRAPH5_aMC@NLO v2.6.5 MC event generator [21]. A $B^{\pm} \to J/\psi K^{\pm} \to e^+e^-K^{\pm}$ MC sample is generated using PYTHIA, interfaced with the EVTGEN v1.6.0 [22] particle decay simulation package. Lastly, $Z \to \mu^+\mu^-\gamma$ events are generated using the POWHEG v2.0 framework with the MiNNLO parton shower scheme [23, 24]. The radiative correction for photons is addressed by PHOTOS v215.5 [25].

All event generators are interfaced with PYTHIA with the CP5 underlying event tune [26] to describe parton showering and hadronization. The NNPDF3.1 set of parton distribution functions is used [27]. The detector response is simulated using the GEANT4 [28] package. The effect of additional proton-proton (pp) interactions in the same or adjacent bunch crossings (pileup) is incorporated into the simulation by including additional pp interactions that have been generated with PYTHIA. The simulated samples are reweighted to reproduce the pileup distribution equivalent to that of the mean number of interactions in data, as measured using the instantaneous luminosity per bunch crossing [29, 30].

4 Merged electron ID

In this section, we discuss the standard PF-based electron reconstruction algorithm and its e_{ME} ID deficiencies. The novel e_{ME} ID is based on electrons reconstructed by the default algorithm, but with additional requirements needed for e_{ME} ID. These selections must be independent of the standard electron ID to provide consistent efficiency across different environments where the signal e_{ME} is well isolated and where the e_{ME} ID efficiency is measured, as described in Section 5. The modifications discussed are the association of a potential secondary track with the EB cluster, modifications of the cluster-track matching, and the use of the boosted decision tree (BDT) method that gives the optimal performance.

4.1 Clustering and primary track selection

The standard EB electron reconstruction is initiated by clustering energy deposits in the ECAL. The clusters are grouped into a supercluster (SC) [1] to incorporate bremsstrahlung photons. Because of the curvature of the electron trajectory in the solenoidal magnetic field, the bremsstrahlung photons increase the size of the cluster in the ϕ direction. Instead of using KF tracks (the default for other particles), electron tracks are reconstructed using an alternative method based on the GSF algorithm. The KF algorithm is a linear least squares estimator, optimal only if the energy loss in the matter is well described by a single Gaussian function of the energy fraction, ζ, retained by the electron after traversing the material. Electron energy losses, however, are dominated by bremsstrahlung production. They follow the Bethe-Heitler distribution, which is highly asymmetric with a singularity at $\zeta \to 1$ and a long tail toward $\zeta = 0$. The GSF algorithm describes the probability density function as a sum of multiple Gaussian functions [18].

Three or four consecutive hits in the pixel detector compatible with the SC position are selected to seed the GSF tracking step. The reconstructed GSF track is associated with the SC using geometrical matching to form an electron candidate [1]. All electron candidates in the EB are considered inputs to the e_{ME} ID. The associated GSF track is considered the primary track for the e_{ME} ID.

The standard electron reconstruction algorithm is suboptimal for e_{ME} for several reasons. If a pair of electrons is as collimated as $\Delta R \equiv \sqrt{(\Delta\eta)^2 + (\Delta\phi)^2} < 0.1$, which is smaller than 13 cm at the center of EB and thus smaller than six times the Molière radius of the lead tungstate crystal, the energy deposit of the two electrons may overlap. If the dielectron is even more boosted, then the SC may fail to resolve the individual energy deposits, affecting the reconstruction of both electron objects and their associated GSF tracks. The GSF algorithm successfully builds two individual GSF tracks in 85% of cases even when the collimation is as small as $\Delta R = 0.01$. However, the shift in the SC's center of gravity (CoG) may cause GSF tracking failure for about 5% of such clusters, which can be recovered by using KF tracks.

As the track of a single charged particle can be reconstructed more than once, the standard track reconstruction has a trajectory "cleaner," which is applied after each iteration of the track finding sequence. When the fraction of shared hits is >19%, the trajectory cleaner removes the track with fewer hits or larger χ^2 if the number of hits is equal [15]. Therefore, if a pair of electrons is extremely boosted with $\gamma_L > 200$, one of the two tracks may be removed by the trajectory cleaner. To recover these events, a single-track e_{ME} that does not require a secondary track is considered, and is discussed in more detail in Section 4.4.

4.2 Secondary track selection

A key variable for distinguishing isolated electrons from e_{ME}'s is the presence of a secondary track. All tracks, either GSF or KF, within $\Delta R < 0.4$ of the electron's GSF track and passing the following track requirements are considered as secondary candidates. For KF tracks, if they are associated with a PF charged hadron, the candidate is required to have its HCAL energy divided by its ECAL energy (H/E) less than 0.1. All secondary track candidates are required to pass quality criteria: $p_T > 10\,\text{GeV}$, the difference between the track origin along the beam axis with that of the primary electron $\Delta z < 0.1\,\text{cm}$, and the number of valid hits $\geq$8, with at least 1 in the pixel detector. KF tracks are also required to pass the standard high-quality track ID criteria ("high-purity" tracks) [15]. These requirements are listed in Table 1. Because most electron tracks are reconstructed by both the KF and GSF algorithms, any KF track lying within $\Delta R < 0.001$ of the GSF primary-electron track is discarded to avoid double counting. Finally, GSF tracks are always preferred over KF tracks when multiple secondary track candidates exist. In addition, vertex fitting based on the KF algorithm [15] is performed by minimizing the mean square error estimated using the primary electron's track and the secondary track candidate. The χ^2 probability of the fit is required to be >1%. If ambiguity remains even within the same type of track collection, the secondary track with a higher vertex fit probability is selected. In the case of background with isolated electrons, secondary tracks passing these criteria mainly arise from bremsstrahlung photons that convert to an e^+e^- pair inside the beam pipe or the first two layers of the pixel detector.

4.3 Modified track-cluster matching

Geometrical matching between the SC and the associated track is a key discriminator between isolated electrons and merged dielectrons. The standard electron ID uses the $\Delta\eta$ between the seed cluster's CoG and the GSF track's position on the EB surface ($\Delta\eta_{in}^{seed}$), where the subscript

Table 1: Secondary track selection criteria

	GSF track	KF track
p_{T}		$>$10 GeV
Δz with the primary track		$<$0.1 cm
Number of valid hits		$\geq$8
Number of valid pixel hits		$\geq$1
Vertex fit probability with the primary track		$>$1%
ΔR	$<$0.4	$0.001 < \Delta R < 0.4$
Track quality	—	High purity
H/E	—	$<$0.1

"in" represents that the track is extrapolated from the innermost track position to the calorimeter surface. Similarly, the $\Delta\phi$ between the SC's CoG and the GSF track's position on the EB surface ($\Delta\phi_{\mathrm{in}}$) is also used. These can yield suboptimal ID performance for e_{ME}, since the overlapping dielectron's energy deposit can displace the CoG. New matching variables that are less sensitive to these effects are devised: Δu, Δv, $\mathrm{cov}^{5\times5}_{i\eta i\eta}$, α_{track}, and $\alpha_{5\times5}$. The variables are defined as shown in Fig. 1. The variable α_{track} denotes the angle between the ϕ axis and the line connecting the extrapolated position of two tracks to the EB surface. Then, a union of the 5×5 matrices of EB crystals ($\mathrm{U}_{5\times5}$) is defined around the closest crystal to the tracks, and its log-weighted CoG is calculated as a weighted average position ($\overline{x}_{\mathrm{U}_{5\times5}}$) using Eq. (2),

$$w_i = \max(0, 4.2 + \ln(E_i/E_{\mathrm{U}_{5\times5}})), \tag{1}$$

$$\overline{x}_{\mathrm{U}_{5\times5}} = \frac{\sum_i^{\mathrm{U}_{5\times5}} w_i x_i}{\sum_i^{\mathrm{U}_{5\times5}} w_i}. \tag{2}$$

A weight (w_i) is defined as Eq. (1), where x_i and E_i represent the position and energy of each crystal within the $\mathrm{U}_{5\times5}$ cluster, and $E_{\mathrm{U}_{5\times5}}$ is the total energy. The weight is chosen to suppress the ECAL noise below 1.5% of $E_{\mathrm{U}_{5\times5}}$, and to have the same CoG if the set of crystals coincides for the $\mathrm{U}_{5\times5}$ cluster and the standard SC. The deviation of this CoG with respect to the electron candidate's track represents the quality of track-cluster matching. The variable Δu (Δv) is defined as an angular separation perpendicular (parallel) to the line defined above. The variable $\alpha_{5\times5}$ is defined as the angle between the ϕ axis and the major axis of the log-weighted distribution of crystal energies calculated with the $\mathrm{U}_{5\times5}$ cluster. The $\mathrm{U}_{5\times5}$ cluster's covariance matrix is expressed by Eq. (3),

$$\mathrm{cov}^{5\times5}_{iaib} = \frac{\sum_i^{\mathrm{U}_{5\times5}} w_i (a_i - \overline{a}_{\mathrm{U}_{5\times5}})(b_i - \overline{b}_{\mathrm{U}_{5\times5}})}{\sum_i^{\mathrm{U}_{5\times5}} w_i}, \tag{3}$$

where a and b can be either η or ϕ axis, and $a_i - \overline{a}_{\mathrm{U}_{5\times5}}$ represents the distance to the ith crystal from the $\mathrm{U}_{5\times5}$ cluster's CoG in units of a crystal.

4.4 The BDT training

The final e_{ME} ID is based on two BDTs: for two-track and single-track candidates. Table 2 (3) lists the variables used to train the two-track (single-track) model. The two-track model mainly uses geometrical matching between two tracks and the $\mathrm{U}_{5\times5}$ cluster's CoG. The key variable for the single-track model is the ratio between the SC energy and the track momentum. Geometrical matching variables between the cluster and the primary track also contribute to a lesser extent.

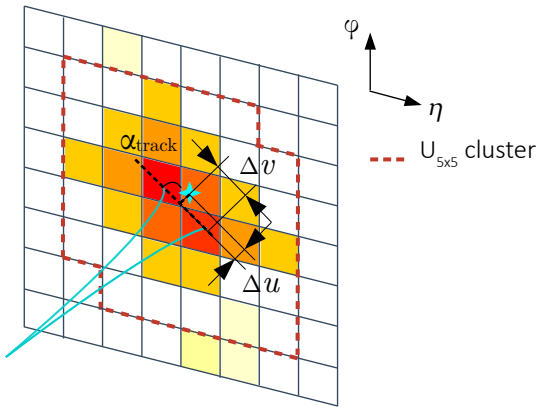

Figure 1: Visual representations of the variables α_{track}, Δu and Δv. Cyan-colored lines depict the incoming tracks of the dielectron. The black dashed line is used to define the u and v directions. The red dashed line represents the $U_{5\times5}$ cluster around the closest crystal from the tracks. The cyan-colored star is the log-weighted CoG of the $U_{5\times5}$ cluster.

Table 2: List of variables used to train the two-track model

Variable	Description
$\Delta v/\Delta R$	Δv divided by ΔR between two tracks
α_{track}	Angle between the line connecting two tracks and the ϕ axis
$\alpha_{5\times5}$	Angle between the major axis of the $U_{5\times5}$ cluster and the ϕ axis
$\Delta\phi_{\text{in}}^{5\times5}$	$\Delta\phi$ between the extrapolated primary track and the CoG of $U_{5\times5}$
$\Delta\eta_{\text{in}}^{5\times5}$	$\Delta\eta$ between the extrapolated primary track and the CoG of $U_{5\times5}$
$\text{cov}_{i\eta i\eta}^{5\times5}$	The log-weighted variance of distances between crystals of $U_{5\times5}$ along the η axis (in units of number of crystals)

The BDTs are trained using merged clusters from $X \to YY \to 4e$ events as signals, and isolated electrons from W boson production, the DY process, and $t\bar{t}$ pair production as background. Preselection criteria are applied. For the $X \to YY \to 4e$ signal hypothesis, at least two reconstructed e_{ME}'s are expected in the event after merging. Accordingly, two electron objects with $p_T > 20\,\text{GeV}$ are required. Both single-track and two-track e_{ME} candidates are required to match a pair of generated electrons within $\Delta R < 0.3$. For the two-track case, the primary and secondary tracks must be located within $\Delta R < 0.001$ of the generated electrons to avoid ambiguity in track matching.

The single-track case mainly occurs when the dielectron has sufficiently high p_T to have a small enough opening angle that the trajectory cleaning feature is used. Therefore, a minimum p_T requirement of 200 GeV is applied to prevent the model from learning the correlation between p_T and other input variables. Also, electrons are required to have $\Delta p_T/p_T < 0.5$, where Δp_T represents the uncertainty in the track's p_T measurement, to avoid learning features reflecting the poorer track momentum description at high energy.

Figure 2 shows distributions of several key ID variables for signal and background events. Data collected with a trigger that requires two SCs with $H/E < 0.15$ and transverse energy (E_T) greater than 60 GeV (2016) or 70 GeV (2017 and 2018) are used, corresponding to an inte-

Table 3: List of variables used to train the single-track model

Variable	Description
E/p	The SC energy divided by the GSF track's momentum
$\Delta\eta_{\text{in}}^{\text{seed}}$	$\Delta\eta$ between the seed cluster and the extrapolated GSF track
$\Delta\phi_{\text{in}}$	$\Delta\phi$ between the SC and the extrapolated GSF track
$E_{1\times5}/E_{5\times5}$	The energy ratio between the arrays of 1×5 and 5×5 crystals (in $\eta\times\phi$)
$\text{cov}_{i\eta i\eta}^{\text{SC}}$	The log-weighted variance of distances between crystals of SC along the η axis (in units of number of crystals)

grated luminosity of $138\,\text{fb}^{-1}$ [29, 31, 32]. The E_{T} is defined as the projection of the vector onto the plane perpendicular to the beam axis, where the vector points to the SC from the interaction point with the magnitude equivalent to the SC's energy. The trigger requirement has no shower shape or track-cluster matching criteria, and it does not bias the ID variable distributions. Corresponding electron p_{T} thresholds are applied for the comparison between data and MC simulation. For e_{ME}, the $\text{U}_{5\times5}$ cluster's CoG should be located between the two tracks, yielding a $\Delta v/\Delta R$ value closer to 0.5. However, single electrons can have a peak close to zero if they have an accidental secondary track that does not deposit energy in the EB. Variables such as α_{track} and $\alpha_{5\times5}$ also contribute to the discrimination, since the decay of a massive particle would produce nonzero recoil momenta along the η axis. The backgrounds, such as converted bremsstrahlung photons, align along the ϕ axis because of the magnetic field. Also, the E/p of an e_{ME} has a higher value, while the background peaks at unity. Lastly, $\Delta\phi_{\text{in}}$ can contribute to the ID even if there is no secondary track because the oppositely charged electron can still shift the SC's CoG in the ϕ direction.

The BDT models are trained using XGBOOST [33] and the model hyperparameters are optimized using HYPEROPT [34]. Simulated events are split into five folds: one is used for testing, and the others for training. The training is repeated for each possible combination of sets, and the model with the largest area under the curve of signal efficiency versus background efficiency is selected. For the two-track model, electrons were reweighted so that the distribution of the E_{T} of their $\text{U}_{5\times5}$ cluster ($E_{\text{T}}^{5\times5}$) is uniform to avoid potential biases due to the different kinematics between background and signal. Figure 3 shows the BDT score distribution for the two-track and single-track models. The threshold on the BDT score is chosen to retain 10% background efficiency, and is approximately 0.6 for both models. Figure 4 shows the dielectron signal ID efficiency as a function of ΔR between the two electrons at several cumulative levels: passing the electron object reconstruction, the secondary track selection, and the e_{ME} ID. The denominator is the number of MC truth dielectrons. The numerator for e_{ME} ID efficiencies requires passing the ID and not being reconstructed as two resolved electrons. The total dielectron efficiency includes the cases where the dielectron is reconstructed as two objects by the standard reconstruction algorithm and where the pair is reconstructed as a single object and passes the e_{ME} ID.

5 Merged electron ID data and MC efficiencies

The e_{ME} ID efficiencies in data are measured for each model. The two-track model efficiency is measured using dielectrons from boosted J/ψ mesons. Events with $\text{J}/\psi\to\text{e}^+\text{e}^-$ candidates are selected from the dataset collected by tagging b hadron decays with muon triggers ("B Parking") [35] and looking for b hadrons from the same pp collision decaying to $\text{J}/\psi+\text{X}$. However,

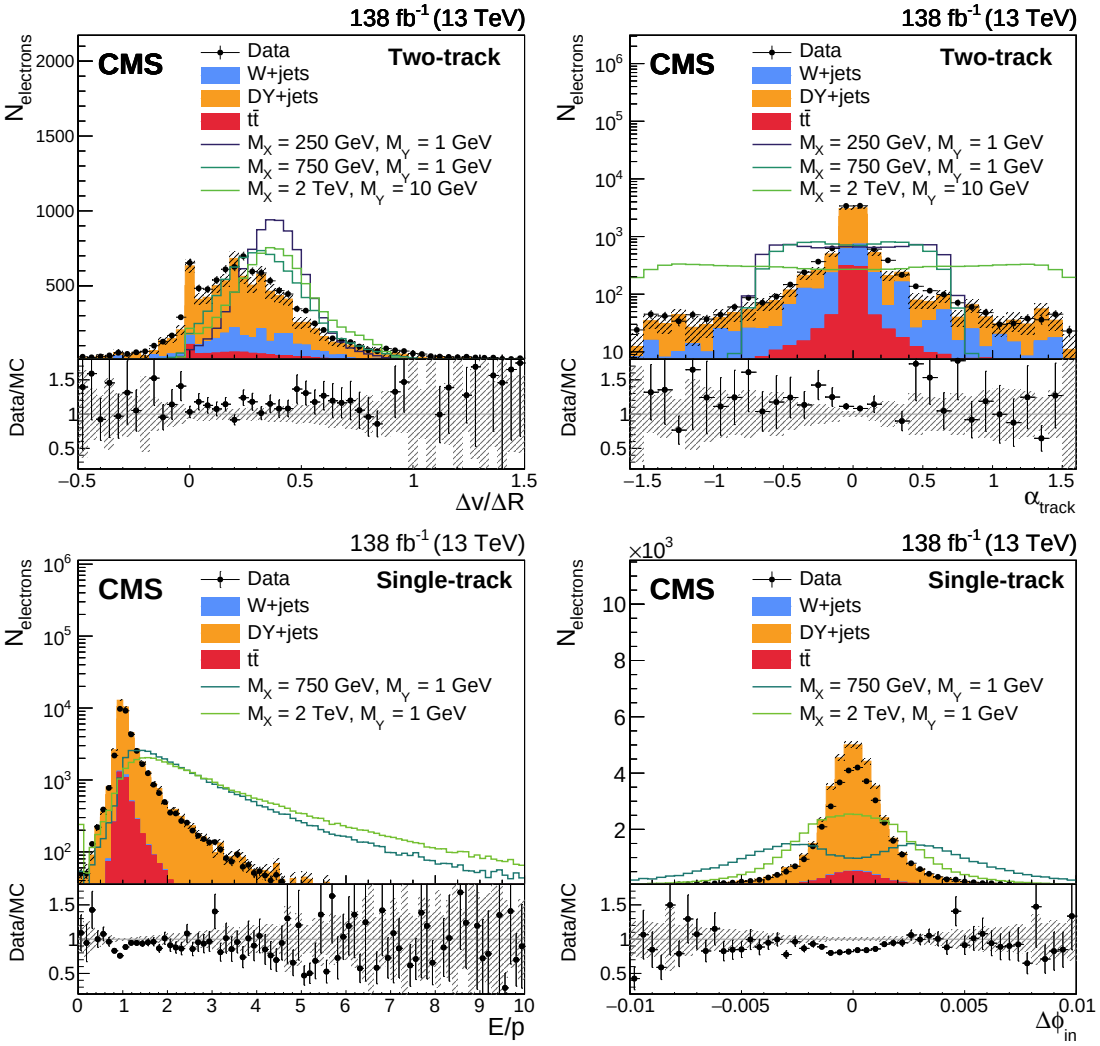

Figure 2: The distribution of the two most contributing variables for the (upper) two-track and (lower) single-track models: (upper left) $\Delta v/\Delta R$, (upper right) α_{track}, (lower left) E/p, and (lower right) $\Delta\phi_{\text{in}}$. The signal samples are displayed according to the resonance masses that match the model. The vertical bar and shaded band represent the statistical uncertainty of the data and MC simulation, respectively. Each lined signal histogram is normalized to the background yield.

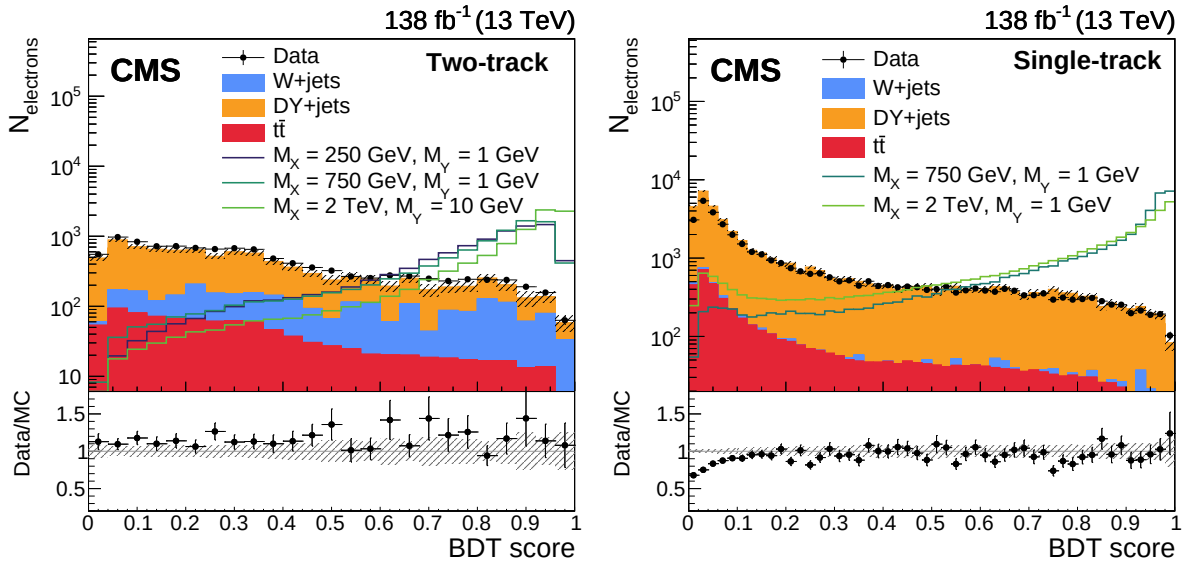

Figure 3: The BDT score distributions of the (left) two-track and (right) single-track models. The signal samples are displayed according to the resonance masses that match the model. The vertical bar and shaded band represent the statistical uncertainty of the data and MC simulation, respectively. Each lined signal histogram is normalized to the background yield.

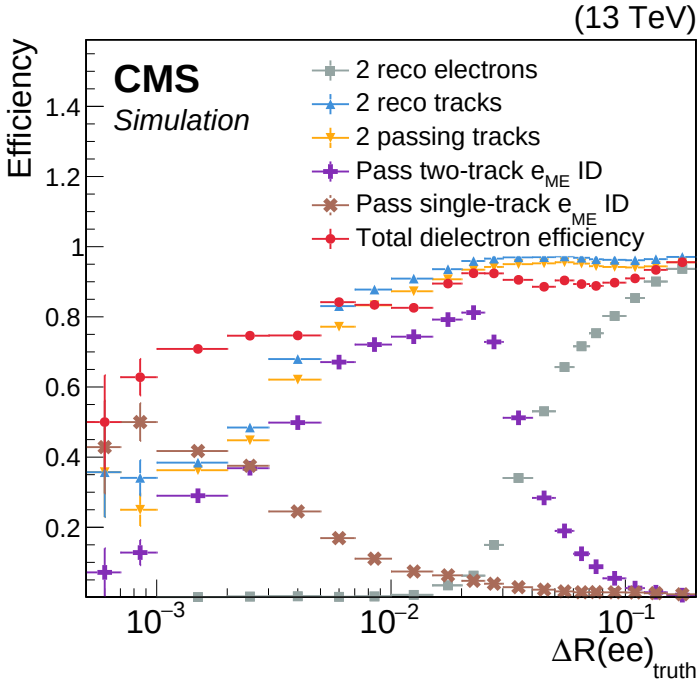

Figure 4: The signal dielectron selection efficiency as a function of ΔR. The vertical error bar represents the statistical uncertainty. An equal number of signal events with $m_X = 250$, 750, 2000 GeV and $m_Y = 1$, 10 GeV are used for each mass point to incorporate dielectrons with various ΔR. The ID efficiencies include the effects of all prerequisite selections. For instance, the e_{ME} ID efficiency with two tracks (purple) includes the efficiency of the track selection described in Table 1 (yellow). The total dielectron efficiency is a sum of the two-track (purple) and single-track (brown) e_{ME} ID efficiencies, and the standard reconstruction efficiency of two electrons (gray).

$J/\psi \to e^+e^-$ decays can only be distinguished from backgrounds by examining the invariant mass of the two electron tracks. Therefore, the single-track model efficiency is estimated using collimated dielectrons from photon conversions where only one of the electron tracks is reconstructed ("single-leg" conversions). The single-leg conversions are identified based on the trajectories' impact parameters and the number of missing hits in the inner tracker [1].

5.1 The two-track model efficiency

Candidate $J/\psi \to e^+e^-$ decays are selected from the B Parking dataset, corresponding to an integrated luminosity of 41.7 fb^{-1}. The events are triggered by a low-p_T muon displaced from the beam axis. The e^+e^- pair originating from the same pp collision as the trigger muon is considered a candidate $J/\psi \to e^+e^-$ decay. Table 4 shows the selection criteria for the $J/\psi \to e^+e^-$ control region. The trigger muon needs to satisfy $p_T > 9\,\text{GeV}$, $|\eta| < 1.5$, and the ratio between the transverse impact parameter in the plane perpendicular to the beam axis (d_{xy}) and its uncertainty must satisfy $d_{xy}/\Delta d_{xy} > 6$. Also, it needs to pass the standard ID criteria optimized for both prompt muons and muons from heavy-flavor decays with medium efficiency ("medium ID") [14]. The $E_T^{5\times5}$ of the e_{ME} candidate must be >20 GeV. The Δz between electron tracks and the trigger muon needs to be <0.1 cm, while the ΔR between them needs to be >0.1 to disambiguate the muon and secondary track. The secondary track must pass the criteria described in Section 4.2. The number of $J/\psi \to e^+e^-$ candidates passing or failing the e_{ME} ID criteria was estimated by fitting the resonance structure in the invariant mass of the two tracks in the range $2.5 < m_{ee} < 4\,\text{GeV}$. Figure 5 shows the dielectron mass distribution of J/ψ candidates with $E_T^{5\times5} > 30\,\text{GeV}$. A Gaussian function is used to describe the nominal signal shape. The nominal background shape is modeled by an exponential function. The e_{ME} ID efficiency is derived using the number of J/ψ candidates that pass the two-track e_{ME} ID divided by the total number of J/ψ candidates. The systematic uncertainty of the fit was evaluated by using alternative signal and background functions. A single-sided Crystal Ball function [36] convoluted with an exponential tail at low masses is used as an alternative signal. The alternative background shape is an exponential decay at high masses and an error function at low masses.

Table 4: Selection criteria for the $J/\psi \to e^+e^-$ control region.

Trigger muon	$p_T > 9\,\text{GeV}$
	$\lvert\eta\rvert < 1.5$
	$d_{xy}/\Delta d_{xy} > 6$
Electron	$E_T^{5\times5} > 20\,\text{GeV}$
	$\lvert\eta_{SC}\rvert < 1.4442$
	$\Delta z(e_1, \mu_{tag}) < 0.1\,\text{cm}$
	$\Delta z(e_2, \mu_{tag}) < 0.1\,\text{cm}$
	$\Delta R(e_2, \mu_{tag}) > 0.1$
	Vertex fit probability >0.01
	$2.5 < m_{ee} < 4.0\,\text{GeV}$

Although boosted $J/\psi \to e^+e^-$ candidates exhibit characteristics similar to the signal e_{ME}, there are also intrinsic differences because most J/ψ mesons are produced from b hadron decays that are displaced from the collision point, and have relatively low momenta. Therefore, the e_{ME} ID efficiency is parametrized as a function of $E_T^{5\times5}$ and the transverse distance (L_{xy}) from the beam

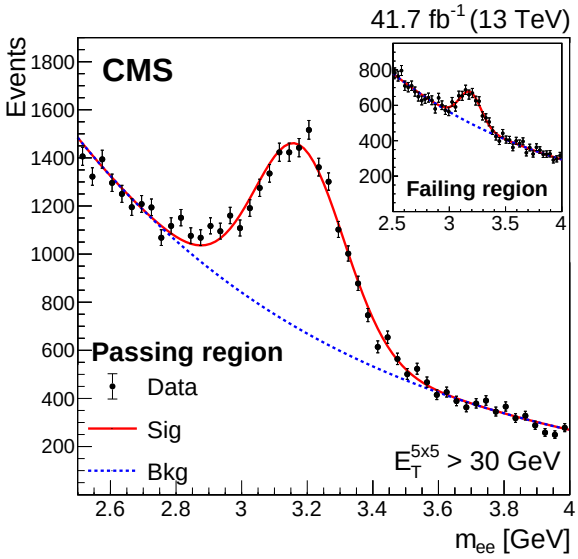

Figure 5: The nominal dielectron mass distribution of J/ψ candidates in the B Parking dataset with $E_{\mathrm{T}}^{5\times5} > 30\,\mathrm{GeV}$ that pass or fail the two-track $\mathrm{e_{ME}}$ ID. The dielectron mass is reconstructed using the tracks of electron candidates.

axis to the vertex. Figure 6 shows the efficiency as a function of $E_{\mathrm{T}}^{5\times5}$ and L_{xy}. The efficiency scale factor (SF) is defined as the ratio between the efficiencies in data and MC simulation, where the MC efficiency is estimated by counting J/ψ candidates. No evident dependence on L_{xy} is observed. To take into account the different $E_{\mathrm{T}}^{5\times5}$ ranges between the boosted J/ψ candidates and various signal mass hypotheses, an $E_{\mathrm{T}}^{5\times5}$-dependent systematic uncertainty in the SF is introduced. The nominal efficiency SF is about 1.03, estimated by averaging over all $E_{\mathrm{T}}^{5\times5}$ bins. The systematic uncertainty is approximately 6% based on the 95% confidence interval ($\mathrm{CI}_{0.95}$), on average. In addition, a fit assuming the SF is linear in $E_{\mathrm{T}}^{5\times5}$ is performed using a first-order polynomial, and the discrepancy with the nominal value is added to the uncertainty in quadrature. From the definition of the efficiency, the SF's systematic variations are not allowed to exceed unity divided by the MC efficiency. The additional uncertainty from the extrapolation covers any potential $E_{\mathrm{T}}^{5\times5}$ dependence of the SF.

5.2 The single-track model efficiency

The ID efficiency of the single-track model is measured using single-leg conversions. The final-state radiation (FSR) in $\mathrm{Z} \to \mu^+\mu^-\gamma$ events is an excellent source of high-purity photons thanks to the low-background environment of the muon final states and $\mathrm{Z} \to \mu^+\mu^-$ background suppression using an invariant mass requirement. Table 5 shows the selection criteria for the single-leg conversion control region. The muons need to have $p_{\mathrm{T}} > 10\,\mathrm{GeV}$, $|\eta| < 2.4$, and pass the medium ID criteria. Isolated single-muon triggers that require $p_{\mathrm{T}} > 24\,(27)\,\mathrm{GeV}$ and $|\eta| < 2.4$ were available during the 2016 and 2018 (2017) data-taking periods, with the total integrated luminosity of $138\,\mathrm{fb}^{-1}$. The p_{T} of a muon that triggers the event must be 2 GeV above the trigger p_{T} threshold to be in the plateau region of the trigger efficiency curve [37]. Also, the muon's tracker isolation must not exceed 10% of the muon p_{T}, where the tracker isolation is defined as the scalar p_{T} sum of all tracks (except the muon's) from the same vertex within $\Delta R < 0.3$ around the muon. As the FSR photon is likely collinear with the muon, the ΔR between the muon that did not trigger the event and the FSR photon must be smaller than 0.8. However, the minimum ΔR between the photon and muons is kept at 0.05 to avoid potential effects due to the energy deposit in ECAL left by the muon. Lastly, the invariant mass of the

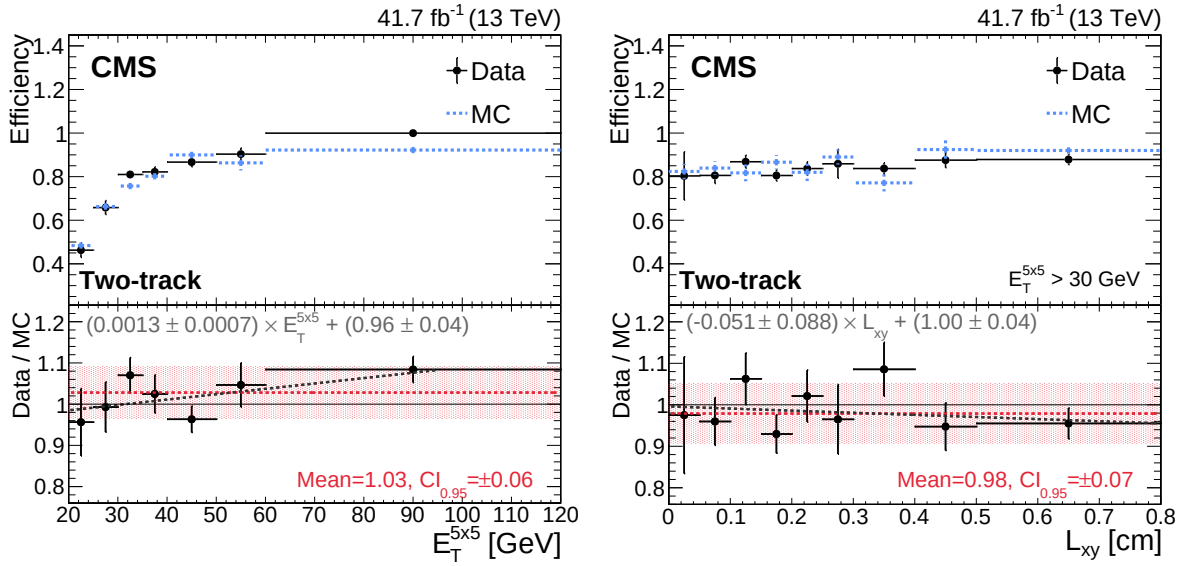

Figure 6: The efficiency and SF for the two-track model as a function of (left) $E_{\mathrm{T}}^{5\times5}$ and (right) L_{xy} with $E_{\mathrm{T}}^{5\times5} > 30\,\mathrm{GeV}$. The vertical bar shows the statistical and systematic uncertainties from the alternative fits, summed in quadrature. The shaded band depicts the $\mathrm{CI}_{0.95}$. The red and gray dashed lines depict the constant and first-order polynomial fits, respectively.

two muons and the photon needs to fulfill $70 < m_{\mu\mu\gamma} < 110\,\mathrm{GeV}$ and $m_{\mu\mu\gamma} + m_{\mu\mu} < 180\,\mathrm{GeV}$ to ensure that the photon originates from FSR.

Table 5: Selection criteria for the $\mathrm{Z} \to \mu^+\mu^-\gamma$ control region.

	Trigger muon (μ_{trig})	FSR muon (μ_{FSR})
Muons	$p_{\mathrm{T}} > 26\,\mathrm{GeV}$ (2016, 2018) $p_{\mathrm{T}} > 29\,\mathrm{GeV}$ (2017)	$p_{\mathrm{T}} > 10\,\mathrm{GeV}$
	$\lvert\eta\rvert < 2.4$	
	$\sum_{\mathrm{tracks}}^{\Delta R<0.3} p_{\mathrm{T}}/p_{\mathrm{T}\mu} < 0.1$	—
Converted photon	$E_{\mathrm{T}}^{5\times5} > 10\,\mathrm{GeV}$	
	$\lvert\eta_{\mathrm{SC}}\rvert < 1.4442$	
	$\Delta R(\mu,\gamma) > 0.05$	
	$\Delta R(\mu_{\mathrm{FSR}},\gamma) < 0.8$	
	$70 < m_{\mu\mu\gamma} < 110\,\mathrm{GeV}$ and $m_{\mu\mu\gamma} + m_{\mu\mu} < 180\,\mathrm{GeV}$	

Figure 7 shows the nominal Z boson candidate mass distribution of $\mu^+\mu^-\gamma$ events in data where the $\mathrm{e}^+\mathrm{e}^-$ pair from the converted photon becomes the e_{ME} candidate. The choice of nominal and alternative signal and background shapes is the same as was used for the two-track model. Analogous to the case with secondary tracks, the efficiency is derived using the number of Z boson candidates that pass the single-track e_{ME} ID divided by the total number of Z candidates. Figure 8 represents the efficiency as a function of $E_{\mathrm{T}}^{5\times5}$ and d_0, where d_0 is the three-dimensional (3D) distance of closest approach (DCA) from the PV to the electron track. No apparent trend is seen in d_0.

Similar to the case with secondary tracks, the final SF is taken from a constant fit of bin-by-

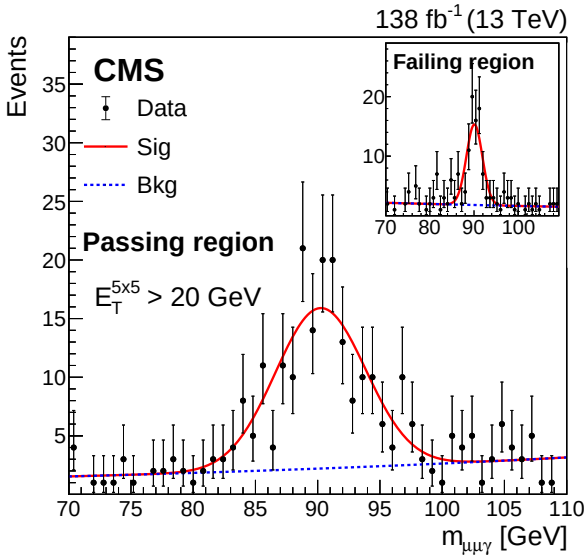

Figure 7: The nominal Z boson candidate mass distribution in data using $\mu^+\mu^-\gamma$ events with $E_{\mathrm{T}}^{5\times5} > 20\,\mathrm{GeV}$. The passing and failing regions represent the Z boson candidate mass distributions with $\mathrm{e_{ME}}$ candidates that pass or fail the $\mathrm{e_{ME}}$ ID.

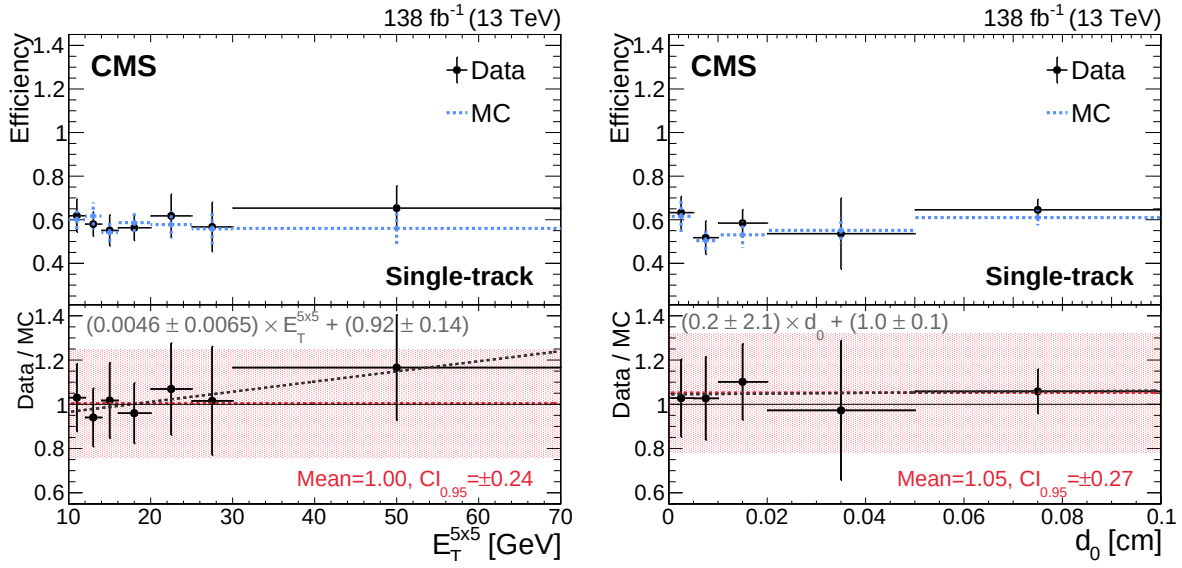

Figure 8: The efficiency and SF as a function of (left) $E_{\mathrm{T}}^{5\times5}$ and (right) d_0 for the single-track model. The vertical bar shows the statistical and systematic uncertainties from the alternative fits, summed in quadrature. The shaded band depicts the $\mathrm{CI}_{0.95}$. The red and gray dashed lines depict the constant and first-order polynomial fits, respectively.

bin SFs. The $CI_{0.95}$ of the fit is assigned as the uncertainty. The SF is found to be unity, but with about 24% uncertainty. The difference between the constant and first-order polynomial fit is added to the uncertainty in quadrature, with an upper bound of unity divided by the MC efficiency. This yields a maximum total uncertainty of approximately 40%. The effect of different topologies between the signal e_{ME} and the converted photon is also assessed. The efficiency in the signal MC sample ranges 65–75% for the single-track case. The efficiency for the $Z \to \mu^+\mu^-\gamma$ events is about 60%. Considering that the observed discrepancy is a result of differences in both $E_T^{5\times5}$ and event topology, and is already well covered by the systematic uncertainty, no additional uncertainty is taken into account.

6 Merged electron energy scale and resolution

The energy of standard electrons, estimated by combining the GSF track momentum and the corresponding SC energy, is dominated by the ECAL measurement for $p_T > 20\,\text{GeV}$ [1]. The single-track e_{ME} is highly collimated, and the standard SC is sufficient to capture all energy deposits from the dielectron. For the two-track e_{ME}, however, the ΔR separation between the electrons ranges from $\mathcal{O}(10^{-2})$ to $\mathcal{O}(10^{-1})$. In this case, the standard SC is not guaranteed to capture all energy deposits from the dielectron. Therefore, the $U_{5\times5}$ cluster's energy is used to describe the e_{ME} energy. The energy scale and resolution of the $U_{5\times5}$ cluster in data can be characterized using a resonance containing a boosted e^+e^- pair as one of the decay products. The $B^\pm \to J/\psi K^\pm \to e^+e^-K^\pm$ decay is an excellent candidate because it is one of the most common b hadron decays containing $J/\psi \to e^+e^-$. Also, the kaon from this decay typically has $1 < p_T < 10\,\text{GeV}$, where the track momentum resolution is about 1% [15] in the barrel region, outperforming the ECAL energy resolution in the range $E_T > 20\,\text{GeV}$. Hence, it is assumed that the resonance shape is determined by the $U_{5\times5}$ cluster. Furthermore, the impact on the Gaussian core of the resonance shape from other contributions, such as $B^\pm \to J/\psi\pi^\pm \to e^+e^-\pi^\pm$ with the wrong mass hypothesis on the track, and the partial reconstruction of $B^0 \to J/\psi K^* \to e^+e^-K^+\pi^-$, is minor when the e^+e^- invariant mass is near the J/ψ mass [38].

Candidate $B^\pm \to J/\psi K^\pm \to e^+e^-K^\pm$ decays are selected using the criteria described in Table 6, in addition to the J/ψ candidate selection in Table 4. A high-purity track with $p_T > 3.5\,\text{GeV}$ and $|\eta| < 2.4$ is selected. Also, the track needs to satisfy Δz with the tag muon $<0.1\,\text{cm}$, but $\Delta R > 0.1$ to disambiguate kaon candidates from the muon. The kaon candidate and electron tracks must form a vertex using the KF algorithm with a probability >1%. The kaon candidate's 3D DCA to the vertex must be $<0.1\,\text{cm}$. The transverse angle between the B meson candidate's momentum and the vector connecting the beam axis and the vertex (α_{2D}) must satisfy $\cos(\alpha_{2D}) > 0.95$. The ΔR between the J/ψ and the kaon candidate needs to be <0.8. The invariant masses of the kaon candidate and each electron are required to be $>2\,\text{GeV}$ to suppress contributions from D meson decays. Finally, the invariant mass of the $U_{5\times5}$ cluster and the kaon candidate must fulfill $4.5 < m(J/\psi, K) < 6\,\text{GeV}$. If multiple B candidates satisfy all criteria for a given e_{ME}, the B candidate with the best vertex fit probability is selected.

Figure 9 shows the invariant mass of the $U_{5\times5}$ cluster and the kaon candidate from data and simulation. The scale and resolution of the B meson resonance are extracted from the signal Crystal Ball function fit's mean and the standard deviation of its Gaussian core. The mean value is 5.231 ± 0.006 (5.232 ± 0.012) GeV, while the standard deviation is 0.050 ± 0.005 (0.053 ± 0.010) GeV in data (simulation). An energy correction to $E_T^{5\times5}$ is introduced to equalize the energy scale and resolution in data and simulation. The energy correction parameters are defined in Eq. (4),

$$E_{T\,\text{corr}}^{5\times5} = \alpha E_T^{5\times5}\left[1 + \text{Gaus}(0, \beta)\right], \tag{4}$$

Table 6: Selection criteria (in addition to Table 4) for the $B^{\pm} \to J/\psi K^{\pm} \to e^{+}e^{-}K^{\pm}$ control region.

kaon	$p_T > 3.5\,\text{GeV}$
	$\lvert\eta\rvert < 2.4$
	High-purity track
	Veto PF electrons and muons
	$\Delta z(K, \mu_{trig}) < 0.1\,\text{cm}$
	$\Delta R(K, \mu_{trig}) > 0.1$
B meson	Vertex fit probability >0.01
	$\text{DCA}(K, \text{vertex}) < 0.1\,\text{cm}$
	$\cos(\alpha_{2D}) > 0.95$
	$\Delta R(J/\psi, K) < 0.8$
	$m(e_1, K) > 2\,\text{GeV}$
	$m(e_2, K) > 2\,\text{GeV}$
	$4.5 < m(J/\psi, K) < 6.0\,\text{GeV}$

where $\text{Gaus}(\mu, \sigma)$ is a Gaussian random number with the mean of μ and the standard deviation of σ. The energy scale correction parameter (α) is estimated by matching the mean of the Crystal Ball function via scaling $E_T^{5\times5}$ in data while fixing the MC shape and other fitted parameters. Likewise, the energy smearing correction parameter (β) is evaluated by equalizing the standard deviation of the Crystal Ball function by smearing $E_T^{5\times5}$ in simulation, while fixing the data shape and other fitted parameters. The optimal values of α and β to equalize the scale and resolution in data and simulation are found to be 1.003 ± 0.003 and 0.02 ± 0.01, respectively. As there are insufficient B candidates to evaluate the correction as a function of $E_T^{5\times5}$, correction parameters are derived inclusively. Therefore, the difference in the $U_{5\times5}$ cluster's energy before and after applying the scaling and smearing correction is assigned as a systematic uncertainty, assuming that the correction parameters are expected to be smaller in higher energy because the $U_{5\times5}$ energy resolution scales proportional to the inverse square root of $E_{U_{5\times5}}$.

7 Summary

Theories of beyond the standard model physics predict light bosons that subsequently decay into a dielectron ($e^{+}e^{-}$). In such models, the light boson can be significantly boosted, and the standard clustering and reconstruction algorithm may fail to resolve the dielectron. The CMS standard electron reconstruction resolves about 5–40% of $e^{+}e^{-}$ pairs when separated by ΔR of 0.02–0.04, corresponding to 1–2 Molière radii, where ΔR is defined as $\Delta R \equiv \sqrt{(\Delta\eta)^2 + (\Delta\phi)^2}$. Moreover, high Lorentz boosts can lead to the absence of either of the electron tracks due to shared hits in the inner tracker. Therefore, novel algorithms to identify merged electrons (e_{ME}) are developed for the single-track and two-track cases, respectively.

The two-track model is trained using a boosted decision tree based on the geometrical compatibility between the merged cluster and the electron tracks. The default clustering algorithm in the electromagnetic calorimeter does not capture all energy deposits from e_{ME} candidates. A cluster consisting of a union of the 5×5 matrices of lead tungstate crystals around the two electron tracks ($U_{5\times5}$) is used to estimate the energy of the e_{ME} instead of the default cluster for

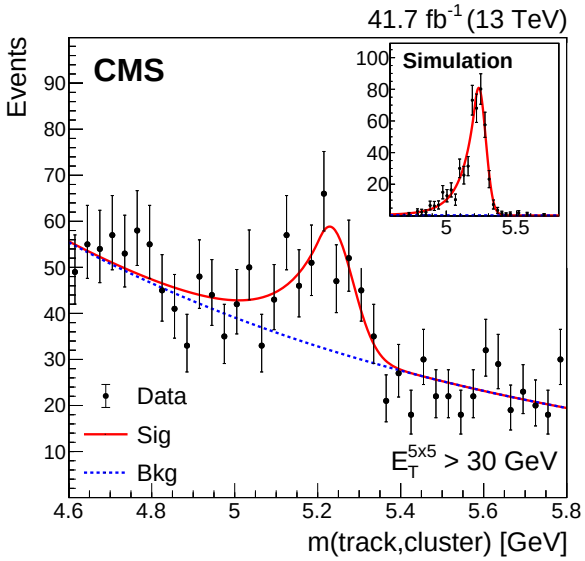

Figure 9: The distribution of the invariant mass between the $U_{5\times5}$ cluster and the kaon candidate with $E_T^{5\times5} > 30\,\text{GeV}$. The vertical bar shows the statistical uncertainty. The signal (background) contribution is modeled with a Crystal Ball (exponential) function, represented with a red (blue) line. The inset on the top right illustrates the mass distribution in a $B^\pm \to J/\psi K^\pm \to e^+e^-K^\pm$ MC sample.

the two-track case. The $U_{5\times5}$ cluster's energy scale and resolution in data are measured with $B^\pm \to J/\psi K^\pm \to e^+e^-K^\pm$ decays by reconstructing the invariant mass of the $U_{5\times5}$ cluster and a track, and found to be consistent with that of the simulation. The two-track model shows about 75% efficiency for the e^+e^- pairs with two reconstructed tracks separated by $\Delta R \simeq 0.01$. The efficiency in data is validated using boosted J/ψ mesons decaying into e^+e^-.

The single-track model targets e^+e^- pairs with an extreme Lorentz boost ($\gamma_L > 200$), and is mainly based on the ratio between the energy of the merged cluster and the reconstructed electron track. Its efficiency is about 50% for the e^+e^- pairs with a single reconstructed track at $\Delta R \simeq 0.001$. The $Z \to \mu^+\mu^-\gamma$ events, where the final-state radiation photon becomes the e^+e^- pair with a single reconstructed track, are used to assess the efficiency in data, which is found to be 60%.

Acknowledgments

We congratulate our colleagues in the CERN accelerator departments for the excellent performance of the LHC and thank the technical and administrative staffs at CERN and at other CMS institutes for their contributions to the success of the CMS effort. In addition, we gratefully acknowledge the computing centers and personnel of the Worldwide LHC Computing Grid and other centers for delivering so effectively the computing infrastructure essential to our analyses. Finally, we acknowledge the enduring support for the construction and operation of the LHC, the CMS detector, and the supporting computing infrastructure provided by the following funding agencies: SC (Armenia), BMBWF and FWF (Austria); FNRS and FWO (Belgium); CNPq, CAPES, FAPERJ, FAPERGS, and FAPESP (Brazil); MES and BNSF (Bulgaria); CERN; CAS, MoST, and NSFC (China); MINCIENCIAS (Colombia); MSES and CSF (Croatia); RIF (Cyprus); SENESCYT (Ecuador); ERC PRG and PSG, TARISTU24-TK10 and MoER TK202 (Estonia); Academy of Finland, MEC, and HIP (Finland); CEA and CNRS/IN2P3 (France); SRNSF

(Georgia); BMFTR, DFG, and HGF (Germany); GSRI (Greece); MATE and NKFIH (Hungary); DAE and DST (India); IPM (Iran); SFI (Ireland); INFN (Italy); MSIT and NRF (Republic of Korea); MES (Latvia); LMTLT (Lithuania); MOE and UM (Malaysia); BUAP, CINVESTAV, CONACYT, LNS, SEP, and UASLP-FAI (Mexico); MOS (Montenegro); MBIE (New Zealand); PAEC (Pakistan); MSHE, NSC, and NAWA (Poland); FCT (Portugal); MESTD (Serbia); MICIU/AEI and PCTI (Spain); MOSTR (Sri Lanka); Swiss Funding Agencies (Switzerland); MST (Taipei); MHESI (Thailand); TUBITAK and TENMAK (Türkiye); NASU (Ukraine); STFC (United Kingdom); DOE and NSF (USA).

Individuals have received support from the Marie-Curie program and the European Research Council and Horizon 2020 Grant, contract Nos. 675440, 724704, 752730, 758316, 765710, 824093, 101115353, 101002207, 101001205, and COST Action CA16108 (European Union); the Leventis Foundation; the Alfred P. Sloan Foundation; the Alexander von Humboldt Foundation; the Science Committee, project no. 22rl-037 (Armenia); the Fonds pour la Formation à la Recherche dans l'Industrie et dans l'Agriculture (FRIA) and Fonds voor Wetenschappelijk Onderzoek contract No. 1228724N (Belgium); the Beijing Municipal Science & Technology Commission, No. Z191100007219010, the Fundamental Research Funds for the Central Universities, the Ministry of Science and Technology of China under Grant No. 2023YFA1605804, the Natural Science Foundation of China under Grant No. 12535004, and USTC Research Funds of the Double First-Class Initiative No. YD2030002017 (China); the Ministry of Education, Youth and Sports (MEYS) of the Czech Republic; the Shota Rustaveli National Science Foundation, grant FR-22-985 (Georgia); the Deutsche Forschungsgemeinschaft (DFG), among others, under Germany's Excellence Strategy – EXC 2121 "Quantum Universe" – 390833306, and under project number 400140256 - GRK2497; the Hellenic Foundation for Research and Innovation (HFRI), Project Number 2288 (Greece); the Hungarian Academy of Sciences, the New National Excellence Program - ÚNKP, the NKFIH research grants K 131991, K 138136, K 143460, K 143477, K 147557, K 146913, K 146914, K 147048, TKP2021-NKTA-64, and 2025-1.1.5-NEMZ_KI-2025-00004, and MATE KKP and KKPCs Research Excellence and Flagship Research Groups grants (Hungary); the Council of Science and Industrial Research, India; ICSC – National Research Center for High Performance Computing, Big Data and Quantum Computing, FAIR – Future Artificial Intelligence Research, and CUP I53D23001070006 (Mission 4 Component 1), funded by the NextGenerationEU program, the Italian Ministry of University and Research (MUR) under Bando PRIN 2022 – CUP I53C24002390006, PRIN PRIMULA 2022RBYK7T (Italy); the Latvian Council of Science; the Ministry of Science and Higher Education, project no. 2022/WK/14, and the National Science Center, contracts Opus 2021/41/B/ST2/01369, 2021/43/B/ST2/01552, 2023/49/B/ST2/03273, and the NAWA contract BPN/PPO/2021/1/00011 (Poland); the Fundação para a Ciência e a Tecnologia (Portugal); the National Priorities Research Program by Qatar National Research Fund; MICIU/AEI/10.13039/501100011033, ERDF/EU, "European Union NextGenerationEU/PRTR", projects PID2022-142604OB-C21, PID2022-139519OB-C21, PID2023-147706NB-I00, PID2023-148896NB-I00, PID2023-146983NB-I00, PID2023-147115NB-I00, PID2023-148418NB-C41, PID2023-148418NB-C42, PID2023-148418NB-C43, PID2023-148418NB-C44, PID2024-158190NB-C22, RYC2021-033305-I, RYC2024-048719-I, CNS2023-144781, CNS2024-154769 and Plan de Ciencia, Tecnología e Innovación de Asturias, Spain; the Chulalongkorn Academic into Its 2nd Century Project Advancement Project, the National Science, Research and Innovation Fund program IND_FF_68_369_2300_097, and the Program Management Unit for Human Resources & Institutional Development, Research and Innovation, grant B39G680009 (Thailand); the Eric & Wendy Schmidt Fund for Strategic Innovation through the CERN Next Generation Triggers project under grant agreement number SIF-2023-004; the Kavli Foundation; the Nvidia Corporation; the SuperMicro Corporation; the Welch Foundation, contract C-1845; and the Weston Havens

Foundation (USA).

References

[1] CMS Collaboration, "Electron and photon reconstruction and identification with the CMS experiment at the CERN LHC", *JINST* **16** (2021) P05014, doi:10.1088/1748-0221/16/05/P05014, arXiv:2012.06888.

[2] V. Barger and H.-S. Lee, "Four-lepton resonance at the Large Hadron Collider", *Phys. Rev. D* **85** (2012) 055030, doi:10.1103/PhysRevD.85.055030, arXiv:1111.0633.

[3] G. C. Branco et al., "Theory and phenomenology of two-Higgs-doublet models", *Phys. Rep.* **516** (2012) 1, doi:10.1016/j.physrep.2012.02.002, arXiv:1106.0034.

[4] D. Curtin, R. Essig, S. Gori, and J. Shelton, "Illuminating dark photons with high-energy colliders", *JHEP* **02** (2015) 157, doi:10.1007/JHEP02(2015)157, arXiv:1412.0018.

[5] CMS Collaboration, "Reconstruction of decays to merged photons using end-to-end deep learning with domain continuation in the CMS detector", *Phys. Rev. D* **108** (2023) 052002, doi:10.1103/PhysRevD.108.052002, arXiv:2204.12313.

[6] CMS Collaboration, "Search for new resonances decaying to pairs of merged diphotons in proton-proton collisions at $\sqrt{s} = 13$ TeV", *Phys. Rev. Lett.* **134** (2025) 041801, doi:10.1103/PhysRevLett.134.041801, arXiv:2405.00834.

[7] ATLAS Collaboration, "A search for new resonances in multiple final states with a high transverse momentum Z boson in $\sqrt{s} = 13$ TeV pp collisions with the ATLAS detector", *JHEP* **06** (2023) 036, doi:10.1007/JHEP06(2023)036, arXiv:2209.15345.

[8] CMS Collaboration, "Search for heavy resonances decaying into four-lepton final states via light bosons in proton-proton collisions at $\sqrt{s}$ = 13 TeV", arXiv:2604.14236. [submitted to Phys. Rev. Lett.].

[9] CMS Collaboration, "The CMS experiment at the CERN LHC", *JINST* **3** (2008) S08004, doi:10.1088/1748-0221/3/08/S08004.

[10] CMS Collaboration, "Development of the CMS detector for the CERN LHC Run 3", *JINST* **19** (2024) P05064, doi:10.1088/1748-0221/19/05/P05064, arXiv:2309.05466.

[11] CMS Collaboration, "Performance of the CMS Level-1 trigger in proton-proton collisions at $\sqrt{s} = 13$ TeV", *JINST* **15** (2020) P10017, doi:10.1088/1748-0221/15/10/P10017, arXiv:2006.10165.

[12] CMS Collaboration, "The CMS trigger system", *JINST* **12** (2017) P01020, doi:10.1088/1748-0221/12/01/P01020, arXiv:1609.02366.

[13] CMS Collaboration, "Performance of the CMS high-level trigger during LHC Run 2", *JINST* **19** (2024) P11021, doi:10.1088/1748-0221/19/11/P11021, arXiv:2410.17038.

[14] CMS Collaboration, "Performance of the CMS muon detector and muon reconstruction with proton-proton collisions at $\sqrt{s} = 13$ TeV", *JINST* **13** (2018) P06015, doi:10.1088/1748-0221/13/06/P06015, arXiv:1804.04528.

[15] CMS Collaboration, "Description and performance of track and primary-vertex reconstruction with the CMS tracker", *JINST* **9** (2014) P10009, doi:10.1088/1748-0221/9/10/P10009, arXiv:1405.6569.

[16] CMS Tracker Group Collaboration, "The CMS Phase-1 pixel detector upgrade", *JINST* **16** (2021) P02027, doi:10.1088/1748-0221/16/02/P02027, arXiv:2012.14304.

[17] CMS Collaboration, "Particle-flow reconstruction and global event description with the CMS detector", *JINST* **12** (2017) P10003, doi:10.1088/1748-0221/12/10/P10003, arXiv:1706.04965.

[18] W. Adam, R. Frühwirth, A. Strandlie, and T. Todorov, "Reconstruction of electrons with the Gaussian-sum filter in the CMS tracker at the LHC", *J. Phys. G* **31** (2005) N9, doi:10.1088/0954-3899/31/9/N01, arXiv:physics/0306087.

[19] CMS Collaboration, "ECAL 2016 refined calibration and Run2 summary plots", CMS Detector Performance Summary CMS-DP-2020-021, 2020.

[20] T. Sjöstrand et al., "An introduction to PYTHIA 8.2", *Comput. Phys. Commun.* **191** (2015) 159, doi:10.1016/j.cpc.2015.01.024, arXiv:1410.3012.

[21] J. Alwall et al., "The automated computation of tree-level and next-to-leading order differential cross sections, and their matching to parton shower simulations", *JHEP* **07** (2014) 79, doi:10.1007/JHEP07(2014)079, arXiv:1405.0301.

[22] D. J. Lange, "The EvtGen particle decay simulation package", *Nucl. Instrum. Methods Phys. Res., Sect. A* **462** (2001) 152, doi:10.1016/S0168-9002(01)00089-4.

[23] P. F. Monni et al., "MiNNLO$_{\text{PS}}$: A new method to match NNLO QCD to parton showers", *JHEP* **05** (2020) 143, doi:10.1007/JHEP05(2020)143, arXiv:1908.06987. [Erratum: doi:10.1007/JHEP02(2022)031].

[24] P. F. Monni, E. Re, and M. Wiesemann, "MiNNLO$_{\text{PS}}$: Optimizing $2 \to 1$ hadronic processes", *Eur. Phys. J. C* **80** (2020) 1075, doi:10.1140/epjc/s10052-020-08658-5, arXiv:2006.04133.

[25] E. Barberio and Z. Wąs, "PHOTOS — a universal Monte Carlo for QED radiative corrections: Version 2.0", *Comput. Phys. Commun.* **79** (1994) 291, doi:10.1016/0010-4655(94)90074-4.

[26] CMS Collaboration, "Extraction and validation of a new set of CMS PYTHIA8 tunes from underlying-event measurements", *Eur. Phys. J. C* **80** (2020) 4, doi:10.1140/epjc/s10052-019-7499-4, arXiv:1903.12179.

[27] R. D. Ball et al., "Parton distributions from high-precision collider data", *Eur. Phys. J. C* **77** (2017) 663, doi:10.1140/epjc/s10052-017-5199-5, arXiv:1706.00428.

[28] GEANT4 Collaboration, "GEANT4—a simulation toolkit", *Nucl. Instrum. Methods Phys. Res., Sect. A* **506** (2003) 250, doi:10.1016/S0168-9002(03)01368-8.

[29] CMS Collaboration, "Precision luminosity measurement in proton-proton collisions at $\sqrt{s} = 13$ TeV in 2015 and 2016 at CMS", *Eur. Phys. J. C* **81** (2021) 800, doi:10.1140/epjc/s10052-021-09538-2, arXiv:2104.01927.

[30] CMS Collaboration, "Pileup mitigation at CMS in 13 TeV data", *JINST* **15** (2020) P09018, doi:10.1088/1748-0221/15/09/P09018, arXiv:2003.00503.

[31] CMS Collaboration, "CMS luminosity measurement for the 2017 data-taking period at $\sqrt{s} = 13$ TeV", CMS Physics Analysis Summary CMS-PAS-LUM-17-004, 2018.

[32] CMS Collaboration, "CMS luminosity measurement for the 2018 data-taking period at $\sqrt{s} = 13$ TeV", CMS Physics Analysis Summary CMS-PAS-LUM-18-002, 2019.

[33] T. Chen and C. Guestrin, "XGBoost: A scalable tree boosting system", in *Proceedings of 22nd ACM SIGKDD International Conference on Knowledge Discovery and Data Mining*, KDD '16, p. 785. 2016. arXiv:1603.02754. doi:10.1145/2939672.2939785.

[34] J. Bergstra, D. Yamins, and D. Cox, "Making a science of model search: Hyperparameter optimization in hundreds of dimensions for vision architectures", in *Proceedings of 30th International Conference on Machine Learning*, volume 28, p. 115. 2013. arXiv:1209.5111.

[35] CMS Collaboration, "Recording and reconstructing 10 billion unbiased B hadron decays in CMS", CMS Detector Performance Summary CMS-DP-2019-043, 2019.

[36] M. Oreglia, "A Study of the Reactions $\psi' \to \gamma\gamma\psi$". Ph.D. thesis, Stanford University, 1980. [SLAC Report SLAC-R-236], see Appendix D.

[37] CMS Collaboration, "Performance of the CMS muon trigger system in proton-proton collisions at $\sqrt{s} = 13$ TeV", *JINST* **16** (2021) P07001, doi:10.1088/1748-0221/16/07/P07001, arXiv:2102.04790.

[38] CMS Collaboration, "Test of lepton flavor universality in $B^{\pm} \to K^{\pm}\mu^{+}\mu^{-}$ and $B^{\pm} \to K^{\pm}e^{+}e^{-}$ decays in proton-proton collisions at $\sqrt{s} = 13$ TeV", *Rep. Prog. Phys.* **87** (2024) 077802, doi:10.1088/1361-6633/ad4e65, arXiv:2401.07090.

A The CMS Collaboration

Yerevan Physics Institute, Yerevan, Armenia
A. Hayrapetyan, V. Makarenko, A. Tumasyan[1]

Institut für Hochenergiephysik, Vienna, Austria
W. Adam, J.W. Andrejkovic, L. Benato, T. Bergauer, M. Dragicevic, C. Giordano, P.S. Hussain, M. Jeitler[2], N. Krammer, A. Li, D. Liko, M. Matthewman, I. Mikulec, J. Schieck[2], R. Schöfbeck[2], D. Schwarz, M. Shooshtari, M. Sonawane, W. Waltenberger, C.-E. Wulz[2]

Universiteit Antwerpen, Antwerpen, Belgium
T. Janssen, H. Kwon, D. Ocampo Henao, T. Van Laer, P. Van Mechelen

Vrije Universiteit Brussel, Brussel, Belgium
J. Bierkens, N. Breugelmans, J. D'Hondt, S. Dansana, A. De Moor, M. Delcourt, F. Heyen, Y. Hong, P. Kashko, S. Lowette, I. Makarenko, D. Müller, J. Song, S. Tavernier, M. Tytgat[3], G.P. Van Onsem, S. Van Putte, D. Vannerom

Université Libre de Bruxelles, Bruxelles, Belgium
B. Bilin, B. Clerbaux, A.K. Das, I. De Bruyn, G. De Lentdecker, H. Evard, L. Favart, P. Gianneios, A. Khalilzadeh, F.A. Khan, A. Malara, M.A. Shahzad, L. Thomas, M. Vanden Bemden, C. Vander Velde, P. Vanlaer, F. Zhang

Ghent University, Ghent, Belgium
M. De Coen, D. Dobur, G. Gokbulut, J. Knolle, D. Marckx, K. Skovpen, A.M. Tomaru, N. Van Den Bossche, J. van der Linden, J. Vandenbroeck, L. Wezenbeek

Université Catholique de Louvain, Louvain-la-Neuve, Belgium
S. Bein, A. Benecke, A. Bethani, G. Bruno, A. Cappati, J. De Favereau De Jeneret, C. Delaere, F. Gameiro Casalinho, A. Giammanco, A.O. Guzel, V. Lemaitre, J. Lidrych, P. Malek, P. Mastrapasqua, S. Turkcapar

Centro Brasileiro de Pesquisas Fisicas, Rio de Janeiro, Brazil
G.A. Alves, M. Barroso Ferreira Filho, E. Coelho, C. Hensel, T. Menezes De Oliveira, C. Mora Herrera, P. Rebello Teles, M. Soeiro, E.J. Tonelli Manganote[4], A. Vilela Pereira[5]

Universidade do Estado do Rio de Janeiro, Rio de Janeiro, Brazil
W.L. Aldá Júnior, H. Brandao Malbouisson, W. Carvalho, J. Chinellato[6], M. Costa Reis, E.M. Da Costa, G.G. Da Silveira[7], D. De Jesus Damiao, S. Fonseca De Souza, R. Gomes De Souza, S. S. Jesus, T. Laux Kuhn[7], M. Macedo, K. Mota Amarilo, L. Mundim, H. Nogima, J.P. Pinheiro, A. Santoro, A. Sznajder, M. Thiel, F. Torres Da Silva De Araujo[8]

Universidade Estadual Paulista, Universidade Federal do ABC, São Paulo, Brazil
C.A. Bernardes[7], F. Damas, T.R. Fernandez Perez Tomei, E.M. Gregores, B. Lopes Da Costa, I. Maietto Silverio, P.G. Mercadante, S.F. Novaes, B. Orzari, Sandra S. Padula, V. Scheurer

Institute for Nuclear Research and Nuclear Energy, Bulgarian Academy of Sciences, Sofia, Bulgaria
A. Aleksandrov, G. Antchev, P. Danev, R. Hadjiiska, P. Iaydjiev, M. Shopova, G. Sultanov

University of Sofia, Sofia, Bulgaria
A. Dimitrov, L. Litov, B. Pavlov, P. Petkov, A. Petrov

Instituto De Alta Investigación, Universidad de Tarapacá, Casilla 7 D, Arica, Chile
S. Keshri, D. Laroze, S. Thakur

Universidad Tecnica Federico Santa Maria, Valparaiso, Chile
W. Brooks

Beihang University, Beijing, China
T. Cheng, T. Javaid, L. Wang, L. Yuan

Department of Physics, Tsinghua University, Beijing, China
Z. Hu, Z. Liang, J. Liu, X. Wang, H. Yang

Institute of High Energy Physics, Beijing, China
G.M. Chen[9], H.S. Chen[9], M. Chen[9], Y. Chen, Q. Hou, X. Hou, F. Iemmi, C.H. Jiang, A. Kapoor[10], H. Liao, G. Liu, Z.-A. Liu[11], J.N. Song[11], S. Song, J. Tao, C. Wang[9], J. Wang, H. Zhang, J. Zhao

State Key Laboratory of Nuclear Physics and Technology, Peking University, Beijing, China
A. Agapitos, Y. Ban, A. Carvalho Antunes De Oliveira, S. Deng, B. Guo, Q. Guo, C. Jiang, A. Levin, C. Li, Q. Li, Y. Mao, S. Qian, S.J. Qian, X. Qin, C. Quaranta, X. Sun, D. Wang, J. Wang, M. Zhang, Y. Zhao, C. Zhou

State Key Laboratory of Nuclear Physics and Technology, Institute of Quantum Matter, South China Normal University, Guangzhou, China
S. Yang

Sun Yat-Sen University, Guangzhou, China
Z. You

University of Science and Technology of China, Hefei, China
K. Jaffel, N. Lu

Nanjing Normal University, Nanjing, China
G. Bauer[12,13], Z. Cui[13], B. Li[14], H. Wang, K. Yi[15], J. Zhang

Institute of Modern Physics and Key Laboratory of Nuclear Physics and Ion-beam Application (MOE) - Fudan University, Shanghai, China
Y. Li

Zhejiang University, Hangzhou, Zhejiang, China
Z. Lin, C. Lu, M. Xiao[16]

Universidad de Los Andes, Bogota, Colombia
C. Avila, D.A. Barbosa Trujillo, A. Cabrera, C. Florez, J. Fraga, J.A. Reyes Vega

Universidad de Antioquia, Medellin, Colombia
C. Rendón, M. Rodriguez, A.A. Ruales Barbosa, J.D. Ruiz Alvarez

University of Split, Faculty of Electrical Engineering, Mechanical Engineering and Naval Architecture, Split, Croatia
N. Godinovic, D. Lelas, A. Sculac

University of Split, Faculty of Science, Split, Croatia
M. Kovac, A. Petkovic, T. Sculac

Institute Rudjer Boskovic, Zagreb, Croatia
P. Bargassa, V. Brigljevic, B.K. Chitroda, D. Ferencek, K. Jakovcic, A. Starodumov, T. Susa

University of Cyprus, Nicosia, Cyprus
A. Attikis, K. Christoforou, C. Leonidou, C. Nicolaou, L. Paizanos, F. Ptochos, P.A. Razis, H. Rykaczewski, H. Saka, A. Stepennov

Charles University, Prague, Czech Republic
M. Finger[†], M. Finger Jr.

Escuela Politecnica Nacional, Quito, Ecuador
E. Ayala

Universidad San Francisco de Quito, Quito, Ecuador
E. Carrera Jarrin

Academy of Scientific Research and Technology of the Arab Republic of Egypt, Egyptian Network of High Energy Physics, Cairo, Egypt
S. Elgammal[17], A. Ellithi Kamel[18]

Center for High Energy Physics (CHEP-FU), Fayoum University, El-Fayoum, Egypt
A. Hussein, H. Mohammed

National Institute of Chemical Physics and Biophysics, Tallinn, Estonia
K. Ehataht, M. Kadastik, T. Lange, C. Nielsen, J. Pata, M. Raidal, N. Seeba, L. Tani

Department of Physics, University of Helsinki, Helsinki, Finland
E. Brücken, A. Milieva, K. Osterberg, M. Voutilainen

Helsinki Institute of Physics, Helsinki, Finland
F. Garcia, P. Inkaew, K.T.S. Kallonen, R. Kumar Verma, T. Lampén, K. Lassila-Perini, B. Lehtela, S. Lehti, T. Lindén, N.R. Mancilla Xinto, M. Myllymäki, M.m. Rantanen, S. Saariokari, N.T. Toikka, J. Tuominiemi

Lappeenranta-Lahti University of Technology, Lappeenranta, Finland
N. Bin Norjoharuddeen, H. Kirschenmann, P. Luukka, H. Petrow

IRFU, CEA, Université Paris-Saclay, Gif-sur-Yvette, France
M. Besancon, F. Couderc, M. Dejardin, D. Denegri, P. Devouge, J.L. Faure, F. Ferri, P. Gaigne, S. Ganjour, P. Gras, G. Hamel de Monchenault, M. Kumar, V. Lohezic, Y. Maidannyk, J. Malcles, F. Orlandi, L. Portales, S. Ronchi, M.Ö. Sahin, A. Savoy-Navarro[19], P. Simkina, M. Titov, M. Tornago

Laboratoire Leprince-Ringuet, CNRS/IN2P3, Ecole Polytechnique, Institut Polytechnique de Paris, Palaiseau, France
R. Amella Ranz, F. Beaudette, G. Boldrini, P. Busson, C. Charlot, M. Chiusi, T.D. Cuisset, O. Davignon, A. De Wit, T. Debnath, I.T. Ehle, S. Ghosh, A. Gilbert, R. Granier de Cassagnac, L. Kalipoliti, M. Manoni, M. Nguyen, S. Obraztsov, C. Ochando, R. Salerno, J.B. Sauvan, Y. Sirois, G. Sokmen, L. Urda Gómez, A. Zabi, A. Zghiche

Université de Strasbourg, CNRS, IPHC UMR 7178, Strasbourg, France
J.-L. Agram[20], J. Andrea, D. Bloch, J.-M. Brom, E.C. Chabert, C. Collard, G. Coulon, S. Falke, U. Goerlach, R. Haeberle, A.-C. Le Bihan, M. Meena,

O. Poncet, G. Saha, P. Vaucelle

Centre de Calcul de l'Institut National de Physique Nucleaire et de Physique des Particules, CNRS/IN2P3, Villeurbanne, France
A. Di Florio

Institut de Physique des 2 Infinis de Lyon (IP2I), Villeurbanne, France
D. Amram, S. Beauceron, B. Blancon, G. Boudoul, N. Chanon, D. Contardo, P. Depasse, H. El Mamouni, J. Fay, S. Gascon, M. Gouzevitch, C. Greenberg, G. Grenier, B. Ille, E. Jourd'Huy, M. Lethuillier, B. Massoteau, L. Mirabito, A. Purohit, M. Vander Donckt, J. Xiao

Georgian Technical University, Tbilisi, Georgia
I. Bagaturia[21], I. Lomidze, Z. Tsamalaidze[22]

RWTH Aachen University, I. Physikalisches Institut, Aachen, Germany
V. Botta, S. Consuegra Rodríguez, L. Feld, K. Klein, M. Lipinski, D. Meuser, P. Nattland, V. Oppenländer, A. Pauls, D. Pérez Adán, N. Röwert, M. Teroerde

RWTH Aachen University, III. Physikalisches Institut A, Aachen, Germany
C. Daumann, S. Diekmann, A. Dodonova, N. Eich, D. Eliseev, F. Engelke, J. Erdmann, M. Erdmann, B. Fischer, T. Hebbeker, K. Hoepfner, F. Ivone, A. Jung, N. Kumar, M.y. Lee, F. Mausolf, M. Merschmeyer, A. Meyer, F. Nowotny, A. Pozdnyakov, W. Redjeb, H. Reithler, U. Sarkar, V. Sarkisovi, A. Schmidt, C. Seth, A. Sharma, J.L. Spah, V. Vaulin, S. Zaleski

RWTH Aachen University, III. Physikalisches Institut B, Aachen, Germany
M.R. Beckers, C. Dziwok, G. Flügge, N. Hoeflich, T. Kress, A. Nowack, O. Pooth, A. Stahl, A. Zotz

Deutsches Elektronen-Synchrotron, Hamburg, Germany
H. Aarup Petersen, A. Abel, M. Aldaya Martin, J. Alimena, S. Amoroso, Y. An, I. Andreev, J. Bach, S. Baxter, M. Bayatmakou, H. Becerril Gonzalez, O. Behnke, A. Belvedere, F. Blekman[23], K. Borras[24], A. Campbell, S. Chatterjee, L.X. Coll Saravia, G. Eckerlin, D. Eckstein, E. Gallo[23], A. Geiser, V. Guglielmi, M. Guthoff, A. Hinzmann, L. Jeppe, M. Kasemann, C. Kleinwort, R. Kogler, M. Komm, D. Krücker, W. Lange, D. Leyva Pernia, K.-Y. Lin, K. Lipka[25], W. Lohmann[26], J. Malvaso, R. Mankel, I.-A. Melzer-Pellmann, M. Mendizabal Morentin, A.B. Meyer, G. Milella, K. Moral Figueroa, A. Mussgiller, L.P. Nair, J. Niedziela, A. Nürnberg, J. Park, E. Ranken, A. Raspereza, D. Rastorguev, L. Rygaard, M. Scham[27,24], S. Schnake[24], P. Schütze, C. Schwanenberger[23], D. Selivanova, K. Sharko, M. Shchedrolosiev, D. Stafford, M. Torkian, F. Vazzoler, A. Ventura Barroso, R. Walsh, D. Wang, Q. Wang, K. Wichmann, L. Wiens[24], C. Wissing, Y. Yang, S. Zakharov, A. Zimermmane Castro Santos

University of Hamburg, Hamburg, Germany
A.R. Alves Andrade, M. Antonello, S. Bollweg, M. Bonanomi, K. El Morabit, Y. Fischer, M. Frahm, E. Garutti, A. Grohsjean, A.A. Guvenli, J. Haller, D. Hundhausen, G. Kasieczka, P. Keicher, R. Klanner, W. Korcari, T. Kramer, C.c. Kuo, F. Labe, J. Lange, A. Lobanov, L. Moureaux, A. Nigamova, K. Nikolopoulos, A. Paasch, K.J. Pena Rodriguez, N. Prouvost, B. Raciti, M. Rieger, D. Savoiu, P. Schleper, M. Schröder, J. Schwandt, M. Sommerhalder, H. Stadie,

G. Steinbrück, R. Ward, B. Wiederspan, M. Wolf

Karlsruher Institut fuer Technologie, Karlsruhe, Germany
S. Brommer, E. Butz, Y.M. Chen, T. Chwalek, A. Dierlamm, G.G. Dincer, U. Elicabuk, N. Faltermann, M. Giffels, A. Gottmann, F. Hartmann[28], M. Horzela, F. Hummer, U. Husemann, J. Kieseler, M. Klute, R. Kunnilan Muhammed Rafeek, O. Lavoryk, J.M. Lawhorn, A. Lintuluoto, S. Maier, M. Mormile, Th. Müller, E. Pfeffer, M. Presilla, G. Quast, K. Rabbertz, B. Regnery, R. Schmieder, N. Shadskiy, I. Shvetsov, H.J. Simonis, L. Sowa, L. Stockmeier, K. Tauqeer, M. Toms, B. Topko, N. Trevisani, C. Verstege, T. Voigtländer, R.F. Von Cube, J. Von Den Driesch, M. Wassmer, R. Wolf, W.D. Zeuner, X. Zuo

Institute of Nuclear and Particle Physics (INPP), NCSR Demokritos, Aghia Paraskevi, Greece
G. Anagnostou, G. Daskalakis, A. Kyriakis

National and Kapodistrian University of Athens, Athens, Greece
G. Melachroinos, Z. Painesis, I. Paraskevas, N. Saoulidou, K. Theofilatos, E. Tziaferi, E. Tzovara, K. Vellidis, I. Zisopoulos

National Technical University of Athens, Athens, Greece
T. Chatzistavrou, G. Karapostoli, K. Kousouris, E. Siamarkou, G. Tsipolitis

University of Ioánnina, Ioánnina, Greece
I. Bestintzanos, I. Evangelou, C. Foudas, P. Katsoulis, P. Kokkas, P.G. Kosmoglou Kioseoglou, N. Manthos, I. Papadopoulos, J. Strologas

HUN-REN Wigner Research Centre for Physics, Budapest, Hungary
D. Druzhkin, C. Hajdu, D. Horvath[29,30], K. Márton, A.J. Rádl[31], F. Sikler, V. Veszpremi

MTA-ELTE Lendület CMS Particle and Nuclear Physics Group, Eötvös Loránd University, Budapest, Hungary
M. Csanád, K. Farkas, A. Fehérkuti[32], M.M.A. Gadallah[33], Á. Kadlecsik, M. León Coello, G. Pásztor, G.I. Veres

Faculty of Informatics, University of Debrecen, Debrecen, Hungary
B. Ujvari, G. Zilizi

HUN-REN ATOMKI - Institute of Nuclear Research, Debrecen, Hungary
G. Bencze, S. Czellar, J. Molnar, Z. Szillasi

Karoly Robert Campus, MATE Institute of Technology, Gyongyos, Hungary
T. Csorgo[32], F. Nemes[32], T. Novak, I. Szanyi[34]

Panjab University, Chandigarh, India
S. Bansal, S.B. Beri, V. Bhatnagar, G. Chaudhary, S. Chauhan, N. Dhingra[35], A. Kaur, A. Kaur, H. Kaur, M. Kaur, S. Kumar, T. Sheokand, J.B. Singh, A. Singla

University of Delhi, Delhi, India
A. Bhardwaj, A. Chhetri, B.C. Choudhary, A. Kumar, A. Kumar, M. Naimuddin, S. Phor, K. Ranjan, M.K. Saini

Indian Institute of Technology Mandi (IIT-Mandi), Himachal Pradesh, India
P. Palni

University of Hyderabad, Hyderabad, India
S. Acharya[36], B. Gomber, B. Sahu[36]

Indian Institute of Technology Kanpur, Kanpur, India
S. Mukherjee

Saha Institute of Nuclear Physics, HBNI, Kolkata, India
S. Bhattacharya, S. Das Gupta, S. Dutta, S. Dutta, S. Sarkar

Indian Institute of Technology Madras, Madras, India
M.M. Ameen, P.K. Behera, S. Chatterjee, G. Dash, A. Dattamunsi, P. Jana, P. Kalbhor, S. Kamble, J.R. Komaragiri[37], T. Mishra, P.R. Pujahari, A.K. Sikdar, R.K. Singh, P. Verma, S. Verma, A. Vijay

IISER Mohali, India, Mohali, India
B.K. Sirasva

Tata Institute of Fundamental Research-A, Mumbai, India
L. Bhatt, S. Dugad, G.B. Mohanty, M. Shelake, P. Suryadevara

Tata Institute of Fundamental Research-B, Mumbai, India
A. Bala, S. Banerjee, S. Barman[38], R.M. Chatterjee, M. Guchait, Sh. Jain, A. Jaiswal, B.M. Joshi, S. Kumar, M. Maity[38], G. Majumder, K. Mazumdar, S. Parolia, R. Saxena, A. Thachayath

National Institute of Science Education and Research, An OCC of Homi Bhabha National Institute, Bhubaneswar, Odisha, India
S. Bahinipati[39], D. Maity[40], P. Mal, K. Naskar[40], A. Nayak[40], S. Nayak, K. Pal, R. Raturi, P. Sadangi, S.K. Swain, S. Varghese[40], D. Vats[40]

Indian Institute of Science Education and Research (IISER), Pune, India
A. Alpana, S. Dube, P. Hazarika, B. Kansal, A. Laha, R. Sharma, S. Sharma, K.Y. Vaish

Indian Institute of Technology Hyderabad, Telangana, India
S. Ghosh

Isfahan University of Technology, Isfahan, Iran
H. Bakhshiansohi[41], A. Jafari[42], V. Sedighzadeh Dalavi, M. Zeinali[43]

Institute for Research in Fundamental Sciences (IPM), Tehran, Iran
S. Bashiri, S. Chenarani[44], S.M. Etesami, Y. Hosseini, M. Khakzad, E. Khazaie, M. Mohammadi Najafabadi, S. Tizchang[45]

University College Dublin, Dublin, Ireland
M. Felcini, M. Grunewald

INFN Sezione di Bari[a], Università di Bari[b], Politecnico di Bari[c], Bari, Italy
M. Abbrescia[a,b], M. Barbieri[a,b], M. Buonsante[a,b], A. Colaleo[a,b], D. Creanza[a,c], N. De Filippis[a,c], M. De Palma[a,b], W. Elmetenawee[a,b,46], N. Ferrara[a,c], L. Fiore[a], L. Longo[a], M. Louka[a,b], G. Maggi[a,c], M. Maggi[a], I. Margjeka[a], V. Mastrapasqua[a,b], S. My[a,b], F. Nenna[a,b], S. Nuzzo[a,b], A. Pellecchia[a,b], A. Pompili[a,b], G. Pugliese[a,c], R. Radogna[a,b], D. Ramos[a], A. Ranieri[a], L. Silvestris[a], F.M. Simone[a,c], Ü. Sözbilir[a], A. Stamerra[a,b], D. Troiano[a,b], R. Venditti[a,b], P. Verwilligen[a], A. Zaza[a,b]

INFN Sezione di Bologna[a], Università di Bologna[b], Bologna, Italy
G. Abbiendi[a], C. Battilana[a,b], D. Bonacorsi[a,b], P. Capiluppi[a,b], F.R. Cavallo[a], M. Cuffiani[a,b], G.M. Dallavalle[a], T. Diotalevi[a,b], F. Fabbri[a], A. Fanfani[a,b], R. Farinelli[a], D. Fasanella[a], C. Grandi[a], S. Lo Meo[a,47], M. Lorusso[a,b], L. Lunerti[a], S. Marcellini[a], G. Masetti[a], F.L. Navarria[a,b], G. Paggi[a,b], A. Perrotta[a], F. Primavera[a,b], A.M. Rossi[a,b], S. Rossi Tisbeni[a,b], T. Rovelli[a,b], G.P. Siroli[a,b]

INFN Sezione di Catania[a], Università di Catania[b], Catania, Italy
S. Costa[a,b,48], A. Di Mattia[a], A. Lapertosa[a], R. Potenza[a,b], A. Tricomi[a,b,48]

INFN Sezione di Firenze[a], Università di Firenze[b], Firenze, Italy
J. Altork[a,b], P. Assiouras[a], G. Barbagli[a], G. Bardelli[a], M. Bartolini[a,b], A. Calandri[a,b], B. Camaiani[a,b], A. Cassese[a], R. Ceccarelli[a], V. Ciulli[a,b], C. Civinini[a], R. D'Alessandro[a,b], L. Damenti[a,b], E. Focardi[a,b], T. Kello[a], G. Latino[a,b], P. Lenzi[a,b], M. Lizzo[a], M. Meschini[a], S. Paoletti[a], A. Papanastassiou[a,b], G. Sguazzoni[a], L. Viliani[a]

INFN Laboratori Nazionali di Frascati, Frascati, Italy
L. Benussi, S. Bianco, S. Meola[49], D. Piccolo

INFN Sezione di Genova[a], Università di Genova[b], Genova, Italy
M. Alves Gallo Pereira[a], F. Ferro[a], E. Robutti[a], S. Tosi[a,b]

INFN Sezione di Milano-Bicocca[a], Università di Milano-Bicocca[b], Milano, Italy
A. Benaglia[a], F. Brivio[a], V. Camagni[a,b], F. Cetorelli[a,b], F. De Guio[a,b], M.E. Dinardo[a,b], P. Dini[a], S. Gennai[a], R. Gerosa[a,b], A. Ghezzi[a,b], P. Govoni[a,b], L. Guzzi[a], M.R. Kim[a], G. Lavizzari[a,b], M.T. Lucchini[a,b], M. Malberti[a], S. Malvezzi[a], A. Massironi[a], D. Menasce[a], L. Moroni[a], M. Paganoni[a,b], S. Palluotto[a,b], D. Pedrini[a], A. Perego[a,b], G. Pizzati[a,b], T. Tabarelli de Fatis[a,b]

INFN Sezione di Napoli[a], Università di Napoli 'Federico II'[b], Napoli, Italy; Università della Basilicata[c], Potenza, Italy; Scuola Superiore Meridionale (SSM)[d], Napoli, Italy
S. Buontempo[a], C. Di Fraia[a,b], F. Fabozzi[a,c], L. Favilla[a,d], A.O.M. Iorio[a,b], L. Lista[a,b,50], P. Paolucci[a,28], B. Rossi[a]

INFN Sezione di Padova[a], Università di Padova[b], Padova, Italy; Universita degli Studi di Cagliari[c], Cagliari, Italy
P. Azzi[a], N. Bacchetta[a,51], D. Bisello[a,b], P. Bortignon[a,c], G. Bortolato[a,b], A.C.M. Bulla[a,c], P. Checchia[a], T. Dorigo[a,52], S. Fantinel[a], F. Gasparini[a,b], U. Gasparini[a,b], S. Giorgetti[a], E. Lusiani[a], M. Margoni[a,b], A.T. Meneguzzo[a,b], J. Pazzini[a,b], P. Ronchese[a,b], R. Rossin[a,b], F. Simonetto[a,b], M. Tosi[a,b], A. Triossi[a,b], S. Ventura[a], M. Zanetti[a,b], P. Zotto[a,b], A. Zucchetta[a,b]

INFN Sezione di Pavia[a], Università di Pavia[b], Pavia, Italy
A. Braghieri[a], S. Calzaferri[a], P. Montagna[a,b], M. Pelliccioni[a], V. Re[a], C. Riccardi[a,b], P. Salvini[a], I. Vai[a,b], P. Vitulo[a,b]

INFN Sezione di Perugia[a], Università di Perugia[b], Perugia, Italy
S. Ajmal[a,b], M.E. Ascioti[a,b], G.M. Bilei[†a], C. Carrivale[a,b], D. Ciangottini[a,b], L. Della Penna[a,b], L. Fanò[a,b], V. Mariani[a,b], M. Menichelli[a], F. Moscatelli[a,53], A. Rossi[a,b], A. Santocchia[a,b], D. Spiga[a], T. Tedeschi[a,b]

INFN Sezione di Pisa[a], Università di Pisa[b], Scuola Normale Superiore di Pisa[c], Pisa, Italy;

Università di Siena[d], Siena, Italy
C. Aimè[a,b], C.A. Alexe[a,c], P. Asenov[a,b], P. Azzurri[a], G. Bagliesi[a], L. Bianchini[a,b], T. Boccali[a], E. Bossini[a], D. Bruschini[a,c], L. Calligaris[a,b], R. Castaldi[a], F. Cattafesta[a,c], M.A. Ciocci[a,d], M. Cipriani[a,b], R. Dell'Orso[a], S. Donato[a,b], R. Forti[a,b], A. Giassi[a], F. Ligabue[a,c], A.C. Marini[a,b], D. Matos Figueiredo[a], A. Messineo[a,b], S. Mishra[a], V.K. Muraleedharan Nair Bindhu[a,b], S. Nandan[a], F. Palla[a], M. Riggirello[a,c], A. Rizzi[a,b], G. Rolandi[a,c], S. Roy Chowdhury[a,54], T. Sarkar[a], A. Scribano[a], P. Solanki[a,b], P. Spagnolo[a], F. Tenchini[a,b], R. Tenchini[a], G. Tonelli[a,b], N. Turini[a,d], F. Vaselli[a,c], A. Venturi[a], P.G. Verdini[a]

INFN Sezione di Roma[a], Sapienza Università di Roma[b], Roma, Italy
P. Akrap[a,b], C. Basile[a,b], S.C. Behera[a], F. Cavallari[a], L. Cunqueiro Mendez[a,b], F. De Riggi[a,b], D. Del Re[a,b], E. Di Marco[a], M. Diemoz[a], F. Errico[a], L. Frosina[a,b], R. Gargiulo[a,b], B. Harikrishnan[a,b], F. Lombardi[a,b], E. Longo[a,b], L. Martikainen[a,b], J. Mijuskovic[a,b], G. Organtini[a,b], N. Palmeri[a,b], R. Paramatti[a,b], S. Rahatlou[a,b], C. Rovelli[a], F. Santanastasio[a,b], L. Soffi[a], V. Vladimirov[a,b]

INFN Sezione di Torino[a], Università di Torino[b], Torino, Italy; Università del Piemonte Orientale[c], Novara, Italy
N. Amapane[a,b], R. Arcidiacono[a,c], S. Argiro[a,b], M. Arneodo[a,c], N. Bartosik[a,c], R. Bellan[a,b], A. Bellora[a,b], C. Biino[a], C. Borca[a,b], N. Cartiglia[a], M. Costa[a,b], R. Covarelli[a,b], N. Demaria[a], L. Finco[a], M. Grippo[a,b], B. Kiani[a,b], L. Lanteri[a,b], F. Legger[a], F. Luongo[a,b], C. Mariotti[a], S. Maselli[a], A. Mecca[a,b], L. Menzio[a,b], P. Meridiani[a], E. Migliore[a,b], M. Monteno[a], M.M. Obertino[a,b], G. Ortona[a], L. Pacher[a,b], N. Pastrone[a], F. Rotondo[a], M. Ruspa[a,c], F. Siviero[a,b], V. Sola[a,b], A. Solano[a,b], C. Tarricone[a,b], D. Trocino[a], G. Umoret[a,b], L. Visca[a,b], R. White[a,b]

INFN Sezione di Trieste[a], Università di Trieste[b], Trieste, Italy
J. Babbar[a,b], S. Belforte[a], V. Candelise[a,b], M. Casarsa[a], F. Cossutti[a], K. De Leo[a], G. Della Ricca[a,b], R. Delli Gatti[a,b]

Kyungpook National University, Daegu, Korea
S. Dogra, J. Hong, J. Kim, T. Kim, D. Lee, H. Lee, J. Lee, S.W. Lee, C.S. Moon, Y.D. Oh, S. Sekmen, B. Tae, Y.C. Yang

Department of Mathematics and Physics - GWNU, Gangneung, Korea
M.S. Kim

Chonnam National University, Institute for Universe and Elementary Particles, Kwangju, Korea
G. Bak, P. Gwak, H. Kim, D.H. Moon, J. Seo

Hanyang University, Seoul, Korea
E. Asilar, F. Carnevali, J. Choi[55], T.J. Kim, Y. Ryou

Korea University, Seoul, Korea
S. Ha, S. Han, B. Hong, J. Kim, K. Lee, K.S. Lee, S. Lee, J. Yoo

Kyung Hee University, Department of Physics, Seoul, Korea
J. Goh, J. Shin, S. Yang

Sejong University, Seoul, Korea
Y. Kang, H. S. Kim, Y. Kim, S. Lee

Seoul National University, Seoul, Korea

J. Almond, J.H. Bhyun, J. Choi, J. Choi, W. Jun, H. Kim, J. Kim, T. Kim, Y. Kim, Y.W. Kim, S. Ko, H. Lee, J. Lee, J. Lee, B.H. Oh, S.B. Oh, J. Shin, U.K. Yang, I. Yoon

University of Seoul, Seoul, Korea
W. Jang, D.Y. Kang, D. Kim, S. Kim, B. Ko, J.S.H. Lee, Y. Lee, I.C. Park, Y. Roh, I.J. Watson

Yonsei University, Department of Physics, Seoul, Korea
G. Cho, K. Hwang, B. Kim, S. Kim, K. Lee, H.D. Yoo

Sungkyunkwan University, Suwon, Korea
Y. Lee, I. Yu

College of Engineering and Technology, American University of the Middle East (AUM), Dasman, Kuwait
T. Beyrouthy, Y. Gharbia

Kuwait University - College of Science - Department of Physics, Safat, Kuwait
F. Alazemi

Riga Technical University, Riga, Latvia
K. Dreimanis, O.M. Eberlins, A. Gaile, C. Munoz Diaz, D. Osite, G. Pikurs, R. Plese, A. Potrebko, M. Seidel, D. Sidiropoulos Kontos

University of Latvia (LU), Riga, Latvia
N.R. Strautnieks

Vilnius University, Vilnius, Lithuania
M. Ambrozas, A. Juodagalvis, S. Nargelas, A. Rinkevicius, G. Tamulaitis

National Centre for Particle Physics, Universiti Malaya, Kuala Lumpur, Malaysia
I. Yusuff[56], Z. Zolkapli

Universidad de Sonora (UNISON), Hermosillo, Mexico
J.F. Benitez, A. Castaneda Hernandez, A. Cota Rodriguez, L.E. Cuevas Picos, H.A. Encinas Acosta, L.G. Gallegos Maríñez, J.A. Murillo Quijada, L. Valencia Palomo

Centro de Investigacion y de Estudios Avanzados del IPN, Mexico City, Mexico
G. Ayala, H. Castilla-Valdez, H. Crotte Ledesma, R. Lopez-Fernandez, J. Mejia Guisao, R. Reyes-Almanza, A. Sánchez Hernández

Universidad Iberoamericana, Mexico City, Mexico
C. Oropeza Barrera, D.L. Ramirez Guadarrama, M. Ramírez García

Benemerita Universidad Autonoma de Puebla, Puebla, Mexico
I. Bautista, F.E. Neri Huerta, I. Pedraza, H.A. Salazar Ibarguen, C. Uribe Estrada

University of Montenegro, Podgorica, Montenegro
I. Bubanja, N. Raicevic

University of Canterbury, Christchurch, New Zealand
P.H. Butler

National Centre for Physics, Quaid-I-Azam University, Islamabad, Pakistan
A. Ahmad, M.I. Asghar, A. Awais, M.I.M. Awan, W.A. Khan

AGH University of Krakow, Krakow, Poland

V. Avati, L. Forthomme, L. Grzanka, M. Malawski, K. Piotrzkowski

National Centre for Nuclear Research, Swierk, Poland
M. Bluj, M. Górski, M. Kazana, M. Szleper, P. Zalewski

Institute of Experimental Physics, Faculty of Physics, University of Warsaw, Warsaw, Poland
K. Bunkowski, K. Doroba, A. Kalinowski, M. Konecki, J. Krolikowski, A. Muhammad

Warsaw University of Technology, Warsaw, Poland
P. Fokow, K. Pozniak, W. Zabolotny

Laboratório de Instrumentação e Física Experimental de Partículas, Lisboa, Portugal
M. Araujo, D. Bastos, C. Beirão Da Cruz E Silva, A. Boletti, M. Bozzo, T. Camporesi, G. Da Molin, M. Gallinaro, J. Hollar, N. Leonardo, G.B. Marozzo, A. Petrilli, M. Pisano, J. Seixas, J. Varela, J.W. Wulff

Faculty of Physics, University of Belgrade, Belgrade, Serbia
P. Adzic, L. Markovic, P. Milenovic, V. Milosevic

VINCA Institute of Nuclear Sciences, University of Belgrade, Belgrade, Serbia
D. Devetak, M. Dordevic, J. Milosevic, L. Nadderd, V. Rekovic, M. Stojanovic

Centro de Investigaciones Energéticas Medioambientales y Tecnológicas (CIEMAT), Madrid, Spain
M. Alcalde Martinez, J. Alcaraz Maestre, Cristina F. Bedoya, J.A. Brochero Cifuentes, Oliver M. Carretero, M. Cepeda, M. Cerrada, N. Colino, B. De La Cruz, A. Delgado Peris, A. Escalante Del Valle, D. Fernández Del Val, J.P. Fernández Ramos, J. Flix, M.C. Fouz, M. Gonzalez Hernandez, O. Gonzalez Lopez, S. Goy Lopez, J.M. Hernandez, M.I. Josa, J. Llorente Merino, C. Martin Perez, E. Martin Viscasillas, D. Moran, C. M. Morcillo Perez, Á. Navarro Tobar, R. Paz Herrera, C. Perez Dengra, A. Pérez-Calero Yzquierdo, J. Puerta Pelayo, I. Redondo, J. Vazquez Escobar

Universidad Autónoma de Madrid, Madrid, Spain
J.F. de Trocóniz

Universidad de Oviedo, Instituto Universitario de Ciencias y Tecnologías Espaciales de Asturias (ICTEA), Oviedo, Spain
B. Alvarez Gonzalez, J. Ayllon Torresano, A. Cardini, J. Cuevas, J. Del Riego Badas, D. Estrada Acevedo, J. Fernandez Menendez, S. Folgueras, I. Gonzalez Caballero, P. Leguina, M. Obeso Menendez, E. Palencia Cortezon, J. Prado Pico, A. Soto Rodríguez, C. Vico Villalba, P. Vischia

Instituto de Física de Cantabria (IFCA), CSIC-Universidad de Cantabria, Santander, Spain
S. Blanco Fernández, I.J. Cabrillo, A. Calderon, J. Duarte Campderros, M. Fernandez, G. Gomez, C. Lasaosa García, R. Lopez Ruiz, C. Martinez Rivero, P. Martinez Ruiz del Arbol, F. Matorras, P. Matorras Cuevas, E. Navarrete Ramos, J. Piedra Gomez, C. Quintana San Emeterio, L. Scodellaro, I. Vila, R. Vilar Cortabitarte, J.M. Vizan Garcia

University of Colombo, Colombo, Sri Lanka
B. Kailasapathy[57], D.D.C. Wickramarathna

University of Ruhuna, Department of Physics, Matara, Sri Lanka

W.G.D. Dharmaratna[58], K. Liyanage, N. Perera

CERN, European Organization for Nuclear Research, Geneva, Switzerland
D. Abbaneo, C. Amendola, R. Ardino, E. Auffray, J. Baechler, D. Barney, J. Bendavid, M. Bianco, A. Bocci, L. Borgonovi, C. Botta, A. Bragagnolo, C.E. Brown, C. Caillol, G. Cerminara, P. Connor, D. d'Enterria, A. Dabrowski, A. David, A. De Roeck, M.M. Defranchis, M. Deile, M. Dobson, P.J. Fernández Manteca, B.A. Fontana Santos Alves, E. Fontanesi, W. Funk, A. Gaddi, S. Giani, D. Gigi, K. Gill, F. Glege, M. Glowacki, A. Gruber, J. Hegeman, J.K. Heikkilä, R. Hofsaess, B. Huber, T. James, P. Janot, O. Kaluzinska, O. Karacheban[26], G. Karathanasis, S. Laurila, P. Lecoq, E. Leutgeb, C. Lourenço, A.-M. Lyon, M. Magherini, L. Malgeri, M. Mannelli, A. Mehta, F. Meijers, J.A. Merlin, S. Mersi, E. Meschi, M. Migliorini, F. Monti, F. Moortgat, M. Mulders, M. Musich, I. Neutelings, S. Orfanelli, F. Pantaleo, M. Pari, G. Petrucciani, A. Pfeiffer, M. Pierini, M. Pitt, H. Qu, D. Rabady, A. Reimers, B. Ribeiro Lopes, F. Riti, P. Rosado, M. Rovere, H. Sakulin, R. Salvatico, S. Sanchez Cruz, S. Scarfi, M. Selvaggi, A. Sharma, K. Shchelina, P. Silva, P. Sphicas[59], A.G. Stahl Leiton, A. Steen, S. Summers, D. Treille, P. Tropea, E. Vernazza, J. Wanczyk[60], S. Wuchterl, M. Zarucki, P. Zehetner, P. Zejdl, G. Zevi Della Porta

PSI Center for Neutron and Muon Sciences, Villigen, Switzerland
T. Bevilacqua[61], L. Caminada[61], W. Erdmann, R. Horisberger, Q. Ingram, H.C. Kaestli, D. Kotlinski, C. Lange, U. Langenegger, L. Noehte[61], T. Rohe, A. Samalan

ETH Zurich - Institute for Particle Physics and Astrophysics (IPA), Zurich, Switzerland
T.K. Aarrestad, M. Backhaus, G. Bonomelli, C. Cazzaniga, K. Datta, P. De Bryas Dexmiers D'Archiacchiac[60], A. De Cosa, G. Dissertori, M. Dittmar, M. Donegà, F. Eble, K. Gedia, F. Glessgen, C. Grab, N. Härringer, T.G. Harte, W. Lustermann, M. Malucchi, R.A. Manzoni, L. Marchese, A. Mascellani[60], F. Nessi-Tedaldi, F. Pauss, V. Perovic, B. Ristic, R. Seidita, J. Steggemann[60], A. Tarabini, D. Valsecchi, R. Wallny

Universität Zürich, Zurich, Switzerland
C. Amsler[62], P. Bärtschi, F. Bilandzija, M.F. Canelli, G. Celotto, K. Cormier, M. Huwiler, W. Jin, A. Jofrehei, B. Kilminster, T.H. Kwok, S. Leontsinis, V. Lukashenko, A. Macchiolo, F. Meng, M. Missiroli, J. Motta, P. Robmann, M. Senger, E. Shokr, F. Stäger, R. Tramontano, P. Viscone

National Central University, Chung-Li, Taiwan
D. Bhowmik, C.M. Kuo, P.K. Rout, S. Taj, P.C. Tiwari[37]

National Taiwan University (NTU), Taipei, Taiwan
L. Ceard, K.F. Chen, Z.g. Chen, A. De Iorio, W.-S. Hou, T.h. Hsu, Y.w. Kao, S. Karmakar, G. Kole, Y.y. Li, R.-S. Lu, E. Paganis, X.f. Su, J. Thomas-Wilsker, L.s. Tsai, D. Tsionou, H.y. Wu, E. Yazgan

High Energy Physics Research Unit, Department of Physics, Faculty of Science, Chulalongkorn University, Bangkok, Thailand
C. Asawatangtrakuldee, N. Srimanobhas

Tunis El Manar University, Tunis, Tunisia
Y. Maghrbi

Çukurova University, Physics Department, Science and Art Faculty, Adana, Turkey
D. Agyel, F. Dolek, I. Dumanoglu[63], Y. Guler[64], E. Gurpinar Guler[64], C. Isik, O. Kara, A. Kayis Topaksu, Y. Komurcu, G. Onengut, K. Ozdemir[65], B. Tali[66], U.G. Tok, E. Uslan, I.S. Zorbakir

Hacettepe University, Ankara, Turkey
S. Sen

Middle East Technical University, Physics Department, Ankara, Turkey
M. Yalvac[67]

Bogazici University, Istanbul, Turkey
B. Akgun, I.O. Atakisi[68], E. Gülmez, M. Kaya[69], O. Kaya[70], M.A. Sarkisla[71], S. Tekten[72]

Istanbul Technical University, Istanbul, Turkey
D. Boncukcu, A. Cakir, K. Cankocak[63,73]

Istanbul University, Istanbul, Turkey
B. Hacisahinoglu, I. Hos[74], B. Kaynak, S. Ozkorucuklu, O. Potok, H. Sert, C. Simsek, C. Zorbilmez

Yildiz Technical University, Istanbul, Turkey
S. Cerci, C. Dozen[75], B. Isildak[76], E. Simsek, D. Sunar Cerci, T. Yetkin[75]

Institute for Scintillation Materials of National Academy of Science of Ukraine, Kharkiv, Ukraine
A. Boyaryntsev, O. Dadazhanova, B. Grynyov

National Science Centre, Kharkiv Institute of Physics and Technology, Kharkiv, Ukraine
L. Levchuk

University of Bristol, Bristol, United Kingdom
J.J. Brooke, A. Bundock, F. Bury, E. Clement, D. Cussans, D. Dharmender, H. Flacher, J. Goldstein, H.F. Heath, M.-L. Holmberg, L. Kreczko, S. Paramesvaran, L. Robertshaw, M.S. Sanjrani[41], J. Segal, V.J. Smith

Rutherford Appleton Laboratory, Didcot, United Kingdom
A.H. Ball, K.W. Bell, A. Belyaev[77], C. Brew, R.M. Brown, D.J.A. Cockerill, A. Elliot, K.V. Ellis, J. Gajownik, K. Harder, S. Harper, J. Linacre, K. Manolopoulos, M. Moallemi, D.M. Newbold, E. Olaiya, D. Petyt, T. Reis, A.R. Sahasransu, G. Salvi, T. Schuh, C.H. Shepherd-Themistocleous, I.R. Tomalin, K.C. Whalen, T. Williams

Imperial College, London, United Kingdom
I. Andreou, R. Bainbridge, P. Bloch, O. Buchmuller, C.A. Carrillo Montoya, D. Colling, I. Das, P. Dauncey, G. Davies, M. Della Negra, S. Fayer, G. Fedi, G. Hall, H.R. Hoorani, A. Howard, G. Iles, C.R. Knight, P. Krueper, J. Langford, K.H. Law, J. León Holgado, L. Lyons, A.-M. Magnan, B. Maier, S. Mallios, A. Mastronikolis, M. Mieskolainen, J. Nash[78], M. Pesaresi, P.B. Pradeep, B.C. Radburn-Smith, A. Richards, A. Rose, L. Russell, K. Savva, C. Seez, R. Shukla, A. Tapper, K. Uchida, G.P. Uttley, T. Virdee[28], M. Vojinovic, N. Wardle, D. Winterbottom

Brunel University, Uxbridge, United Kingdom

J.E. Cole, A. Khan, P. Kyberd, I.D. Reid

Baylor University, Waco, Texas, USA
S. Abdullin, A. Brinkerhoff, E. Collins, M.R. Darwish, J. Dittmann, K. Hatakeyama, V. Hegde, J. Hiltbrand, B. McMaster, J. Samudio, S. Sawant, C. Sutantawibul, J. Wilson

Bethel University, St. Paul, Minnesota, USA
J.M. Hogan

Catholic University of America, Washington, DC, USA
R. Bartek, A. Dominguez, S. Raj, A.E. Simsek, S.S. Yu

The University of Alabama, Tuscaloosa, Alabama, USA
B. Bam, A. Buchot Perraguin, S. Campbell, R. Chudasama, S.I. Cooper, C. Crovella, G. Fidalgo, S.V. Gleyzer, A. Khukhunaishvili, K. Matchev, E. Pearson, C.U. Perez, P. Rumerio[79], E. Usai, R. Yi

Boston University, Boston, Massachusetts, USA
S. Cholak, G. De Castro, Z. Demiragli, C. Erice, C. Fangmeier, C. Fernandez Madrazo, J. Fulcher, F. Golf, S. Jeon, J. O'Cain, I. Reed, J. Rohlf, K. Salyer, D. Sperka, D. Spitzbart, I. Suarez, A. Tsatsos, E. Wurtz, A.G. Zecchinelli

Brown University, Providence, Rhode Island, USA
G. Barone, G. Benelli, D. Cutts, S. Ellis, L. Gouskos, M. Hadley, U. Heintz, K.W. Ho, T. Kwon, L. Lambrecht, G. Landsberg, K.T. Lau, J. Luo, S. Mondal, J. Roloff, T. Russell, S. Sagir[80], X. Shen, M. Stamenkovic, N. Venkatasubramanian

University of California, Davis, Davis, California, USA
S. Abbott, S. Baradia, B. Barton, R. Breedon, H. Cai, M. Calderon De La Barca Sanchez, E. Cannaert, M. Chertok, M. Citron, J. Conway, P.T. Cox, R. Erbacher, O. Kukral, G. Mocellin, S. Ostrom, I. Salazar Segovia, J.S. Tafoya Vargas, W. Wei, S. Yoo

University of California, Los Angeles, California, USA
K. Adamidis, M. Bachtis, D. Campos, R. Cousins, A. Datta, G. Flores Avila, J. Hauser, M. Ignatenko, M.A. Iqbal, T. Lam, Y.f. Lo, E. Manca, A. Nunez Del Prado, D. Saltzberg, V. Valuev

University of California, Riverside, Riverside, California, USA
R. Clare, J.W. Gary, G. Hanson

University of California, San Diego, La Jolla, California, USA
A. Aportela, A. Arora, J.G. Branson, S. Cittolin, S. Cooperstein, B. D'Anzi, D. Diaz, J. Duarte, L. Giannini, Y. Gu, J. Guiang, V. Krutelyov, R. Lee, J. Letts, H. Li, M. Masciovecchio, F. Mokhtar, S. Mukherjee, M. Pieri, D. Primosch, M. Quinnan, V. Sharma, M. Tadel, E. Vourliotis, F. Würthwein, A. Yagil, Z. Zhao

University of California, Santa Barbara - Department of Physics, Santa Barbara, California, USA
A. Barzdukas, L. Brennan, C. Campagnari, S. Carron Montero[81], K. Downham, C. Grieco, M.M. Hussain, J. Incandela, M.W.K. Lai, A.J. Li, P. Masterson, J. Richman, S.N. Santpur, U. Sarica, R. Schmitz, F. Setti, J. Sheplock, D. Stuart,

T.Á. Vámi, X. Yan, D. Zhang

California Institute of Technology, Pasadena, California, USA
A. Albert, S. Bhattacharya, A. Bornheim, O. Cerri, R. Kansal, J. Mao, H.B. Newman, G. Reales Gutiérrez, T. Sievert, M. Spiropulu, J.R. Vlimant, R.A. Wynne, S. Xie

Carnegie Mellon University, Pittsburgh, Pennsylvania, USA
J. Alison, S. An, M. Cremonesi, V. Dutta, E.Y. Ertorer, T. Ferguson, T.A. Gómez Espinosa, A. Harilal, A. Kallil Tharayil, M. Kanemura, C. Liu, M. Marchegiani, P. Meiring, T. Mudholkar, S. Murthy, P. Palit, K. Park, M. Paulini, A. Roberts, A. Sanchez, W. Terrill

University of Colorado Boulder, Boulder, Colorado, USA
J.P. Cumalat, W.T. Ford, A. Hart, S. Kwan, J. Pearkes, C. Savard, N. Schonbeck, K. Stenson, K.A. Ulmer, S.R. Wagner, N. Zipper, D. Zuolo

Cornell University, Ithaca, New York, USA
J. Alexander, X. Chen, J. Dickinson, A. Duquette, J. Fan, X. Fan, J. Grassi, S. Hogan, P. Kotamnives, J. Monroy, G. Niendorf, M. Oshiro, J.R. Patterson, A. Ryd, J. Thom, P. Wittich, R. Zou, L. Zygala

Fermi National Accelerator Laboratory, Batavia, Illinois, USA
M. Albrow, M. Alyari, O. Amram, G. Apollinari, A. Apresyan, L.A.T. Bauerdick, D. Berry, J. Berryhill, P.C. Bhat, K. Burkett, J.N. Butler, A. Canepa, G.B. Cerati, H.W.K. Cheung, F. Chlebana, C. Cosby, G. Cummings, I. Dutta, V.D. Elvira, J. Freeman, A. Gandrakota, Z. Gecse, L. Gray, D. Green, A. Grummer, S. Grünendahl, D. Guerrero, O. Gutsche, R.M. Harris, T.C. Herwig, J. Hirschauer, V. Innocente, B. Jayatilaka, S. Jindariani, M. Johnson, U. Joshi, B. Klima, K.H.M. Kwok, S. Lammel, C. Lee, D. Lincoln, R. Lipton, T. Liu, K. Maeshima, D. Mason, P. McBride, P. Merkel, S. Mrenna, S. Nahn, J. Ngadiuba, D. Noonan, S. Norberg, V. Papadimitriou, N. Pastika, K. Pedro, C. Pena[82], C.E. Perez Lara, F. Ravera, A. Reinsvold Hall[83], L. Ristori, M. Safdari, E. Sexton-Kennedy, N. Smith, A. Soha, L. Spiegel, S. Stoynev, J. Strait, L. Taylor, S. Tkaczyk, N.V. Tran, L. Uplegger, E.W. Vaandering, C. Wang, I. Zoi

University of Florida, Gainesville, Florida, USA
C. Aruta, P. Avery, D. Bourilkov, P. Chang, V. Cherepanov, R.D. Field, C. Huh, E. Koenig, M. Kolosova, J. Konigsberg, A. Korytov, G. Mitselmakher, K. Mohrman, A. Muthirakalayil Madhu, N. Rawal, S. Rosenzweig, V. Sulimov, Y. Takahashi, J. Wang

Florida State University, Tallahassee, Florida, USA
T. Adams, A. Al Kadhim, A. Askew, S. Bower, R. Goff, R. Hashmi, A. Hassani, R.S. Kim, T. Kolberg, G. Martinez, M. Mazza, H. Prosper, P.R. Prova, R. Yohay

Florida Institute of Technology, Melbourne, Florida, USA
B. Alsufyani, S. Butalla, S. Das, M. Hohlmann, M. Lavinsky, E. Yanes

University of Illinois Chicago, Chicago, Illinois, USA
M.R. Adams, N. Barnett, A. Baty, C. Bennett, R. Cavanaugh, R. Escobar Franco, O. Evdokimov, C.E. Gerber, H. Gupta, M. Hawksworth, A. Hingrajiya, D.J. Hofman, Z. Huang, J.h. Lee, C. Mills, S. Nanda, G. Nigmatkulov, B. Ozek, T. Phan, D. Pilipovic, R. Pradhan, E. Prifti, P. Roy, T. Roy, N. Singh, M.B. Tonjes, N. Varelas, M.A. Wadud, J. Yoo

The University of Iowa, Iowa City, Iowa, USA
M. Alhusseini, D. Blend, K. Dilsiz[84], O.K. Köseyan, A. Mestvirishvili[85], O. Neogi, H. Ogul[86], Y. Onel, A. Penzo, C. Snyder, E. Tiras[87]

Johns Hopkins University, Baltimore, Maryland, USA
B. Blumenfeld, J. Davis, A.V. Gritsan, L. Kang, S. Kyriacou, P. Maksimovic, M. Roguljic, S. Sekhar, M.V. Srivastav, M. Swartz

The University of Kansas, Lawrence, Kansas, USA
A. Abreu, L.F. Alcerro Alcerro, J. Anguiano, S. Arteaga Escatel, P. Baringer, A. Bean, R. Bhattacharya, Z. Flowers, D. Grove, J. King, G. Krintiras, M. Lazarovits, C. Le Mahieu, J. Marquez, M. Murray, M. Nickel, S. Popescu[88], C. Rogan, C. Royon, S. Rudrabhatla, S. Sanders, C. Smith, G. Wilson

Kansas State University, Manhattan, Kansas, USA
B. Allmond, N. Islam, A. Ivanov, K. Kaadze, Y. Maravin, J. Natoli, G.G. Reddy, D. Roy, G. Sorrentino

University of Maryland, College Park, Maryland, USA
A. Baden, A. Belloni, J. Bistany-riebman, S.C. Eno, N.J. Hadley, S. Jabeen, R.G. Kellogg, T. Koeth, B. Kronheim, S. Lascio, P. Major, A.C. Mignerey, C. Palmer, C. Papageorgakis, M.M. Paranjpe, E. Popova[89], A. Shevelev, L. Zhang

Massachusetts Institute of Technology, Cambridge, Massachusetts, USA
C. Baldenegro Barrera, H. Bossi, S. Bright-Thonney, I.A. Cali, Y.c. Chen, P.c. Chou, M. D'Alfonso, J. Eysermans, C. Freer, G. Gomez-Ceballos, M. Goncharov, G. Grosso, P. Harris, D. Hoang, G.M. Innocenti, K. Ivanov, D. Kovalskyi, J. Krupa, L. Lavezzo, Y.-J. Lee, K. Long, C. Mcginn, A. Novak, M.I. Park, C. Paus, C. Reissel, C. Roland, G. Roland, S. Rothman, T.a. Sheng, G.S.F. Stephans, D. Walter, J. Wang, Z. Wang, B. Wyslouch, T. J. Yang

University of Minnesota, Minneapolis, Minnesota, USA
B. Crossman, W.J. Jackson, C. Kapsiak, M. Krohn, D. Mahon, J. Mans, B. Marzocchi, R. Rusack, O. Sancar, R. Saradhy, N. Strobbe

University of Nebraska-Lincoln, Lincoln, Nebraska, USA
K. Bloom, D.R. Claes, G. Haza, J. Hossain, C. Joo, I. Kravchenko, A. Rohilla, J.E. Siado, W. Tabb, A. Vagnerini, A. Wightman, F. Yan

State University of New York at Buffalo, Buffalo, New York, USA
H. Bandyopadhyay, L. Hay, H.w. Hsia, I. Iashvili, A. Kalogeropoulos, A. Kharchilava, A. Mandal, M. Morris, D. Nguyen, S. Rappoccio, H. Rejeb Sfar, A. Williams, P. Young, D. Yu

Northeastern University, Boston, Massachusetts, USA
G. Alverson, E. Barberis, J. Bonilla, B. Bylsma, M. Campana, J. Dervan, Y. Haddad, Y. Han, I. Israr, A. Krishna, M. Lu, N. Manganelli, R. Mccarthy, D.M. Morse, T. Orimoto, L. Skinnari, C.S. Thoreson, E. Tsai, D. Wood

Northwestern University, Evanston, Illinois, USA
S. Dittmer, K.A. Hahn, M. Mcginnis, Y. Miao, D.G. Monk, M.H. Schmitt, A. Taliercio, M. Velasco, J. Wang

University of Notre Dame, Notre Dame, Indiana, USA
G. Agarwal, R. Band, R. Bucci, S. Castells, A. Das, A. Ehnis, R. Goldouzian,

M. Hildreth, K. Hurtado Anampa, T. Ivanov, C. Jessop, A. Karneyeu, K. Lannon, J. Lawrence, N. Loukas, L. Lutton, J. Mariano, N. Marinelli, I. Mcalister, T. McCauley, C. Mcgrady, C. Moore, Y. Musienko[22], H. Nelson, M. Osherson, A. Piccinelli, R. Ruchti, A. Townsend, Y. Wan, M. Wayne, H. Yockey

The Ohio State University, Columbus, Ohio, USA
A. Basnet, M. Carrigan, R. De Los Santos, L.S. Durkin, C. Hill, M. Joyce, M. Nunez Ornelas, D.A. Wenzl, B.L. Winer, B. R. Yates

Princeton University, Princeton, New Jersey, USA
H. Bouchamaoui, G. Dezoort, P. Elmer, A. Frankenthal, M. Galli, B. Greenberg, N. Haubrich, K. Kennedy, G. Kopp, Y. Lai, D. Lange, A. Loeliger, D. Marlow, I. Ojalvo, J. Olsen, F. Simpson, D. Stickland, C. Tully

University of Puerto Rico, Mayaguez, Puerto Rico, USA
S. Malik, R. Sharma

Purdue University, West Lafayette, Indiana, USA
S. Chandra, R. Chawla, A. Gu, L. Gutay, M. Jones, A.W. Jung, D. Kondratyev, M. Liu, G. Negro, N. Neumeister, G. Paspalaki, S. Piperov, N.R. Saha, J.F. Schulte, F. Wang, A. Wildridge, W. Xie, Y. Yao, Y. Zhong

Purdue University Northwest, Hammond, Indiana, USA
N. Parashar, A. Pathak, E. Shumka

Rice University, Houston, Texas, USA
D. Acosta, A. Agrawal, C. Arbour, T. Carnahan, P. Das, K.M. Ecklund, S. Freed, F.J.M. Geurts, T. Huang, I. Krommydas, N. Lewis, W. Li, J. Lin, O. Miguel Colin, B.P. Padley, R. Redjimi, J. Rotter, M. Wulansatiti, E. Yigitbasi, Y. Zhang

University of Rochester, Rochester, New York, USA
O. Bessidskaia Bylund, A. Bodek, P. de Barbaro†, R. Demina, A. Garcia-Bellido, H.S. Hare, O. Hindrichs, N. Parmar, P. Parygin[89], H. Seo, R. Taus

Rutgers, The State University of New Jersey, Piscataway, New Jersey, USA
B. Chiarito, J.P. Chou, S.V. Clark, S. Donnelly, D. Gadkari, Y. Gershtein, E. Halkiadakis, C. Houghton, D. Jaroslawski, A. Kobert, S. Konstantinou, I. Laflotte, A. Lath, J. Martins, M. Perez Prada, B. Rand, J. Reichert, P. Saha, S. Salur, S. Schnetzer, S. Somalwar, R. Stone, S.A. Thayil, S. Thomas, J. Vora

University of Tennessee, Knoxville, Tennessee, USA
D. Ally, A.G. Delannoy, S. Fiorendi, J. Harris, T. Holmes, A.R. Kanuganti, N. Karunarathna, J. Lawless, L. Lee, E. Nibigira, B. Skipworth, S. Spanier

Texas A&M University, College Station, Texas, USA
D. Aebi, M. Ahmad, T. Akhter, K. Androsov, A. Bolshov, O. Bouhali[90], A. Cagnotta, V. D'Amante, R. Eusebi, P. Flanagan, J. Gilmore, Y. Guo, T. Kamon, S. Luo, R. Mueller, A. Safonov

Texas Tech University, Lubbock, Texas, USA
N. Akchurin, J. Damgov, Y. Feng, N. Gogate, Y. Kazhykarim, K. Lamichhane, S.W. Lee, C. Madrid, A. Mankel, T. Peltola, I. Volobouev

Vanderbilt University, Nashville, Tennessee, USA
E. Appelt, Y. Chen, S. Greene, A. Gurrola, W. Johns, R. Kunnawalkam Elayavalli,

A. Melo, D. Rathjens, F. Romeo, P. Sheldon, S. Tuo, J. Velkovska, J. Viinikainen, J. Zhang

University of Virginia, Charlottesville, Virginia, USA
B. Cardwell, H. Chung, B. Cox, J. Hakala, G. Hamilton Ilha Machado, R. Hirosky, M. Jose, A. Ledovskoy, C. Mantilla, C. Neu, C. Ramón Álvarez, Z. Wu

Wayne State University, Detroit, Michigan, USA
S. Bhattacharya, P.E. Karchin

University of Wisconsin - Madison, Madison, Wisconsin, USA
A. Aravind, S. Banerjee, K. Black, T. Bose, E. Chavez, S. Dasu, P. Everaerts, C. Galloni, H. He, M. Herndon, A. Herve, C.K. Koraka, S. Lomte, R. Loveless, A. Mallampalli, A. Mohammadi, S. Mondal, T. Nelson, G. Parida, L. Pétré, D. Pinna, A. Savin, V. Shang, V. Sharma, W.H. Smith, D. Teague, H.F. Tsoi, W. Vetens, A. Warden

Authors affiliated with an international laboratory covered by a cooperation agreement with CERN
S. Afanasiev, V. Alexakhin, Yu. Andreev, T. Aushev, D. Budkouski, R. Chistov, M. Danilov, T. Dimova, A. Ershov, S. Gninenko, I. Gorbunov, A. Gribushin, A. Kamenev, V. Karjavine, M. Kirsanov, V. Klyukhin, O. Kodolova[91], V. Korenkov, I. Korsakov, A. Kozyrev, N. Krasnikov, A. Lanev, A. Malakhov, V. Matveev, A. Nikitenko[92,91], V. Palichik, V. Perelygin, S. Petrushanko, S. Polikarpov, O. Radchenko, M. Savina, V. Shalaev, S. Shmatov, S. Shulha, Y. Skovpen, K. Slizhevskiy, V. Smirnov, O. Teryaev, I. Tlisova, A. Toropin, N. Voytishin, A. Zarubin, I. Zhizhin

Authors affiliated with an institute formerly covered by a cooperation agreement with CERN
L. Dudko, V. Kim[22], V. Murzin, V. Oreshkin, D. Sosnov, E. Boos, V. Bunichev, M. Dubinin[82], V. Savrin, A. Snigirev

†: Deceased
[1]Also at Yerevan State University, Yerevan, Armenia
[2]Also at TU Wien, Vienna, Austria
[3]Also at Ghent University, Ghent, Belgium
[4]Also at FACAMP - Faculdades de Campinas, Sao Paulo, Brazil
[5]Also at Universidade do Estado do Rio de Janeiro, Rio de Janeiro, Brazil
[6]Also at Universidade Estadual de Campinas, Campinas, Brazil
[7]Also at Federal University of Rio Grande do Sul, Porto Alegre, Brazil
[8]Also at The University of the State of Amazonas, Manaus, Brazil
[9]Also at University of Chinese Academy of Sciences, Beijing, China
[10]Also at China Center of Advanced Science and Technology, Beijing, China
[11]Also at University of Chinese Academy of Sciences, Beijing, China
[12]Also at School of Physics, Zhengzhou University, Zhengzhou, China
[13]Now at Henan Normal University, Xinxiang, China
[14]Also at University of Shanghai for Science and Technology, Shanghai, China
[15]Now at The University of Iowa, Iowa City, Iowa, USA
[16]Also at Center for High Energy Physics, Peking University, Beijing, China
[17]Now at British University in Egypt, Cairo, Egypt
[18]Now at Cairo University, Cairo, Egypt
[19]Also at Purdue University, West Lafayette, Indiana, USA

[20]Also at Université de Haute Alsace, Mulhouse, France
[21]Also at Ilia State University, Tbilisi, Georgia
[22]Also at an institute formerly covered by a cooperation agreement with CERN
[23]Also at University of Hamburg, Hamburg, Germany
[24]Also at RWTH Aachen University, III. Physikalisches Institut A, Aachen, Germany
[25]Also at Bergische University Wuppertal (BUW), Wuppertal, Germany
[26]Also at Brandenburg University of Technology, Cottbus, Germany
[27]Also at Forschungszentrum Jülich, Juelich, Germany
[28]Also at CERN, European Organization for Nuclear Research, Geneva, Switzerland
[29]Also at HUN-REN ATOMKI - Institute of Nuclear Research, Debrecen, Hungary
[30]Now at Universitatea Babes-Bolyai - Facultatea de Fizica, Cluj-Napoca, Romania
[31]Also at MTA-ELTE Lendület CMS Particle and Nuclear Physics Group, Eötvös Loránd University, Budapest, Hungary
[32]Also at HUN-REN Wigner Research Centre for Physics, Budapest, Hungary
[33]Also at Physics Department, Faculty of Science, Assiut University, Assiut, Egypt
[34]Also at The University of Kansas, Lawrence, Kansas, USA
[35]Also at Punjab Agricultural University, Ludhiana, India
[36]Also at University of Hyderabad, Hyderabad, India
[37]Also at Indian Institute of Science (IISc), Bangalore, India
[38]Also at University of Visva-Bharati, Santiniketan, India
[39]Also at IIT Bhubaneswar, Bhubaneswar, India
[40]Also at Institute of Physics, Bhubaneswar, India
[41]Also at Deutsches Elektronen-Synchrotron, Hamburg, Germany
[42]Also at Isfahan University of Technology, Isfahan, Iran
[43]Also at Sharif University of Technology, Tehran, Iran
[44]Also at Department of Physics, University of Science and Technology of Mazandaran, Behshahr, Iran
[45]Also at Department of Physics, Faculty of Science, Arak University, ARAK, Iran
[46]Also at Helwan University, Cairo, Egypt
[47]Also at Italian National Agency for New Technologies, Energy and Sustainable Economic Development, Bologna, Italy
[48]Also at Centro Siciliano di Fisica Nucleare e di Struttura Della Materia, Catania, Italy
[49]Also at Università degli Studi Guglielmo Marconi, Roma, Italy
[50]Also at Scuola Superiore Meridionale, Università di Napoli 'Federico II', Napoli, Italy
[51]Also at Fermi National Accelerator Laboratory, Batavia, Illinois, USA
[52]Also at Lulea University of Technology, Lulea, Sweden
[53]Also at Consiglio Nazionale delle Ricerche - Istituto Officina dei Materiali, Perugia, Italy
[54]Also at UPES - University of Petroleum and Energy Studies, Dehradun, India
[55]Also at Institut de Physique des 2 Infinis de Lyon (IP2I), Villeurbanne, France
[56]Also at Department of Applied Physics, Faculty of Science and Technology, Universiti Kebangsaan Malaysia, Bangi, Malaysia
[57]Also at Trincomalee Campus, Eastern University, Sri Lanka, Nilaveli, Sri Lanka
[58]Also at Saegis Campus, Nugegoda, Sri Lanka
[59]Also at National and Kapodistrian University of Athens, Athens, Greece
[60]Also at Ecole Polytechnique Fédérale Lausanne, Lausanne, Switzerland
[61]Also at Universität Zürich, Zurich, Switzerland
[62]Also at Stefan Meyer Institute for Subatomic Physics, Vienna, Austria
[63]Also at Near East University, Research Center of Experimental Health Science, Mersin, Turkey

[64]Also at Konya Technical University, Konya, Turkey
[65]Also at Izmir Bakircay University, Izmir, Turkey
[66]Also at Adiyaman University, Adiyaman, Turkey
[67]Also at Bozok Universitetesi Rektörlügü, Yozgat, Turkey
[68]Also at Istanbul Sabahattin Zaim University, Istanbul, Turkey
[69]Also at Marmara University, Istanbul, Turkey
[70]Also at Milli Savunma University, Istanbul, Turkey
[71]Also at Informatics and Information Security Research Center, Gebze/Kocaeli, Turkey
[72]Also at Kafkas University, Kars, Turkey
[73]Now at Istanbul Okan University, Istanbul, Turkey
[74]Also at Istanbul University - Cerrahpasa, Faculty of Engineering, Istanbul, Turkey
[75]Also at Istinye University, Istanbul, Turkey
[76]Also at Yildiz Technical University, Istanbul, Turkey
[77]Also at School of Physics and Astronomy, University of Southampton, Southampton, United Kingdom
[78]Also at Monash University, Faculty of Science, Clayton, Australia
[79]Also at Università di Torino, Torino, Italy
[80]Also at Karamanoğlu Mehmetbey University, Karaman, Turkey
[81]Also at California Lutheran University, Thousand Oaks, California, USA
[82]Also at California Institute of Technology, Pasadena, California, USA
[83]Also at United States Naval Academy, Annapolis, Maryland, USA
[84]Also at Bingol University, Bingol, Turkey
[85]Also at Georgian Technical University, Tbilisi, Georgia
[86]Also at Sinop University, Sinop, Turkey
[87]Also at Erciyes University, Kayseri, Turkey
[88]Also at Horia Hulubei National Institute of Physics and Nuclear Engineering (IFIN-HH), Bucharest, Romania
[89]Now at another institute formerly covered by a cooperation agreement with CERN
[90]Also at Hamad Bin Khalifa University (HBKU), Doha, Qatar
[91]Also at Yerevan Physics Institute, Yerevan, Armenia
[92]Also at Imperial College, London, United Kingdom